REPORT DOCUMENTATION PAGE

Form Approved
OMB No. 0704-0188

1. AGENCY USE ONLY (Leave blank)	2. REPORT DATE	3. REPORT TYPE AND DATES COVERED
		FINAL REPORT 15 Sep 92 - 14 Jan 95

4. TITLE AND SUBTITLE
Photorefractive Mode Conversion for Fault-Tolerant Source-Fiber Coupling

5. FUNDING NUMBERS
~~XXXXXXXX~~
ARPA
61101E
8723/03

6. AUTHOR(S)
Arthur E-T Chiou
Program Manager
Rockwell International Corporation

7. PERFORMING ORGANIZATION NAME(S) AND ADDRESS(ES)
Rockwell International Corporation
1049 Camino Dos Rios
Thousand Oaks, CA 91358

8. PERFORMING ORGANIZATION REPORT NUMBER
AFOSR-TR- 95-0377

9. SPONSORING / MONITORING AGENCY NAME(S) AND ADDRESS(ES)
AFOSR/NE
110 Duncan Avenue Suite B115
Bolling AFB DC 20332-0001

10. SPONSORING / MONITORING AGENCY REPORT NUMBER
F49620-92-C-0067

11. SUPPLEMENTARY NOTES

12a. DISTRIBUTION / AVAILABILITY STATEMENT
APPROVED FOR PUBLIC RELEASE: DISTRIBUTION UNLIMITED

12b. DISTRIBUTION CODE

13. ABSTRACT *(Maximum 200 words)*

The purpose of this contract is to study the potential applications of nonlinear optical phenomena in photorefractive materials in various geometries (such as waveguides, fibers, and bulks) for efficient and fault-tolerant laser-to-fiber coupling. The study focuses on the development of new application concepts, theoretical modeling and experimental demonstration/characterization of novel devices based on energy coupling among different optical modes via dynamic holograms in c-axis photorefractive waveguides and fibers; and on optical resonators incorporating photorefractive dynamic holograms in bulk crystals. The holograms are self-generated by the interaction of various optical modes (waves) propagating through the photorefractive material. The final objective is to identify an optimum material and configuration and to demonstrate a higher coupling efficiency and better fault-tolerance in coupling light from a laser to an optical fiber or waveguide than that achievable by the conventional method.

14. SUBJECT TERMS			15. NUMBER OF PAGES
			16. PRICE CODE
17. SECURITY CLASSIFICATION OF REPORT	18. SECURITY CLASSIFICATION OF THIS PAGE	19. SECURITY CLASSIFICATION OF ABSTRACT	20. LIMITATION OF ABSTRACT
UNCLASSIFIED	UNCLASSIFIED	UNCLASSIFIED	UNCLASSIFIED

Photrefractive Mode Conversion for Fault-tolerant Source-fiber Coupling

SC71074.FTR

Final Technical Report

September 15, 1992 thru January 14, 1995

Prepared for:
AFOSR/Directorate of Physics and Electronics
Building 410
Bolling AFB, DC 20332-6448
Attn: Dr. Alan Craig

Prepared by:
A. Chiou, Principal Investigator
Rockwell Science Center
1049 Camino Dos Rios
Thousand Oaks, CA 91360

April 1995

Sponsored by Defense Advanced Research Projects Agency

DARPA Order No. 8723

Monitored by AFOSR Under Contract No. F49620-92-C-0067

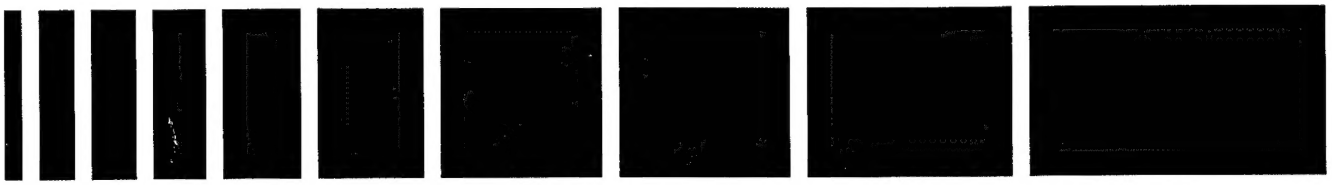

Rockwell

Science Center

Copy # 4

Table of Contents

Page

1.0 Summary 1

1.1 Contract Description 1
1.2 Scientific Problem 1
1.3 Progress and Accomplishments 4
1.4 Publications and Presentations 4
1.5 Technical Disclosure 5

2.0 Technical Discussion 6

2.1 A Brief Introduction to Photorefraction 6
2.2 Photorefractive Two-wave Mixing 7
2.3 Photorefractive Phase Conjugate Resonator 8
2.4 Mutually Pumped Phase Conjugation (MPPC) 12

3.0 Progress 15

3.1 Laser-to-Fiber Coupling Using a Semilinear Phase Conjugate Resonator (SPCR) 16
3.2 A Photorefractive Spatial Mode Converter for Multimode to Singlemode Fiber Optic Coupling 24

4.0 Suggestion for Further Research and Development 30
5.0 References 32
6.0 Appendix 38

List of Figures

Figure		Page
1	Approximate spectral range of some selected photorefractive materials.....	7
2	A qualitative explanation of enrage transfer in photorefractive two-beam coupling in terms of the constructive (or destructive) interference of the transmitted and the diffractive components of two interacting beams.....	8
3	(a) Geometrical representation of wave-vectors associated with higher order and lower order modes in a multimode waveguide; (b) a conceptual illustration of spatial mode conversion in a c-axis oriented photorefractive waveguide	9
4	An illustration of beam fanning effect in a barium titanate sample.....	10
5	A schematic illustration of a (a) linear phase conjugate resonator (LPCR), and (b) semilinear phase conjugate resonator (SPCR)	11
6	A schematic illustration of mutually-pumped phase conjugation (MPPC).....	13
7	A schematic illustration of the spatial mode conversion and efficient coupling of the output of a multimode fiber into a single mode fiber.....	14
8	Experimental configuration of a semilinear phase conjugate resonator (SPCR) using a 50% beam splitter and a variable aperture as the output coupler. BS: beam splitter, FL: focusing lens, OC: output coupler, VA: variable aperture, D: detector	17
9	Experimental results showing the decay and the self-recovery of the oscillation in SPCR (see Fig. 8) when the output coupler was rotated (by about 1° along the vertical axis) from the optimum position. The top and the bottom traces represent the transmitted and the phase conjugate signals, respectively.....	17
10	The coupling efficiency (▲) and the amplification factors (■) of the SPCR as a function of the verticular angular position of the output coupler.....	18
11	Intensity distribution at the output of SPCR using a 40mm diameter chromium circular disk on glass as the output coupler (a) prior to oscillation buildup, (b) when the oscillation reaches a steady state	19
12	Experimental configuration for fault-tolerant laser-to-fiber coupling using SPCR	19
13	Experimental results showing fault-tolerant coupling. The upper and the lower traces correspond to output signals from detectors D1 and D2, (i.e., the transmitted and the phase conjugate signals), respectively	21
14	Techniques for optimizing the optical feedback from the fiber to maximize the coupling efficiency	22

List of Figures (Cont'd)

Figure		Page
15	Theoretical result showing the optical transmission of the SPCR as a function of the photorefractive coupling strength (ΓL) with the reflectance of the output coupler as a varying parameter	23
16	A comparison of the current performance and the projected improved performance of SPCR to that of the conventional approach for laser-to-fiber coupling in terms of the coupling efficiency as a function of lateral misalignment (normalized to fiber core diameter)	23
17	An experimental configuration for the demonstration of fault-tolerant and efficient coupling of light from a multimode fiber into a singlemode fiber. λ/2: half-wave plate, PBS: polarizing beam splitter, SH: shutter, BS: beam splitter, D: detector, MO: microscope objective, FH: fiber holder, SMF: singlemode fiber, MMF: multimode fiber, M: mirror, BT: barium titanate crystal, L: lens, BB: beam blockage, P: polarizer	25
18	Multimode to singlemode light coupling efficiency as a function of the power ratio of the beacon and the signal beams	26
19	Oscillograms showing the decay and the recovery of the signal transmitted through the singlemode fiber when the beacon beam was switched off and on again at an instant when the transmitted power was (a) 54%, (b) 0.01% of the peak value.	27
20	Oscillograms showing the modulated signal transmitted into the SMF from the MMF; (a) at steady-state oscillation, (b) when the beacon beam was switched off and the photorefractive gratings were completely erased	27
21	Oscillograms showing the abrupt drop and the gradual recovery of the signal transmitted through the singlemode fiber when the fiber facet was displaced (a) horizontally, (b) vertically. The minima of the signal level represent the background due to back reflection of the beacon beam from the microscope objective and the fiber	28
22	A plot of coupling efficiency as a function of the number of modes for the comparison of the performance of multimode-to-singlemode fiber optic coupling using the conventional techniques vs the photorefractive approach based on MPPC	29

1.0 Summary

1.1 Contract Description

The purpose of this contract is to study the potential applications of nonlinear optical phenomena in photorefractive materials in various geometries (such as waveguides, fibers, and bulks) for efficient and fault-tolerant laser-to-fiber coupling. The study focuses on the development of new application concepts, theoretical modeling and experimental demonstration/characterization of novel devices based on energy coupling among different optical modes via dynamic holograms in c-axis photorefractive waveguides and fibers; and on optical resonators incorporating photorefractive dynamic holograms in bulk crystals. The holograms are self-generated by the interaction of various optical modes (waves) propagating through the photorefractive material. The final objective is to identify an optimum material and configuration and to demonstrate a higher coupling efficiency and better fault-tolerance in coupling light from a laser to an optical fiber or waveguide than that achievable by the conventional method.

1.2 Scientific Problem

The conventional approaches using passive optics to improve the coupling efficiency in coupling light from a laser diode to a single-mode optical fiber or waveguide impose extremely stringent requirement on alignment. A small misalignment due to any external factors such as temperature change or material fatigue can lead to significant reduction in the coupling efficiency. Spatial mode conversion in photorefractive materials offer the potential of adaptively modifying the dynamic holograms (generated by the optical waves) to achieve high coupling efficiency and to reduce the sensitivity to misalignment.

Three novel device concepts for fault-tolerant coupling were conceived and/or demonstrated during the course of this program. Each of these concepts is based on a unique photorefractive phenomenon in a specific geometry/configuration; namely 1) Higher order to lower order spatial mode conversion in photorefractive fibers and waveguides; 2) Free-propagating mode to guided mode conversion in a self-pumped semilinear resonator; and 3) Multimode to singlemode conversion based on mutually pumped phase conjugation.

1.2.1 Spatial Mode Conversion in Photorefractive Fibers and Waveguides

It is well-known that strong energy coupling via two-wave mixing occurs in photorefractive crystals such as barium titanate ($BaTiO_3$), strontium barium niobate (SBN), bismuth silicon oxide (BSO), and gallium arsenide (GaAs). Under appropriate conditions, a weak beam can be amplified at the expense of a strong pump beam. This nonreciprocal energy transfer has been used for many applications including coherent image amplifier, energy efficient optical interconnection, and laser beam cleanup. The same concept can be used for spatial mode conversion in photorefractive crystal fibers. In principle, when an optical wave is launched into a c-axis photorefractive fiber, energy can be transferred from higher order to lower order modes (or vice versa, depending on the direction of propagation with respect to the positive c-axis) as a result of the formation of self-induced dynamic gratings. The efficiency of spatial mode conversion depends on the optical property of the material as well as the geometrical parameters of the waveguide. A thorough understanding of the dependence via theoretical modeling and experimental characterization is indispensable to the enhancement of spatial mode conversion and to the design of an optimum structure for energy efficient and fault-tolerant laser-to-fiber coupler. During the course of this program, we have identified a photorefractive core/cladding design structure that potentially minimizes the loss and maximizes the mode conversion efficiency.

1.2.2 Spatial Mode Conversion from a Free-Propagating (Gaussian) Mode to Guided Modes Using a Photorefractive Semilinear Resonators

When a laser beam with an appropriate wavelength and polarization enters a photorefractive crystal, the intensity distribution of the beam at the exit face of the crystal usually exhibits a characteristic fan shape. Such a phenomenon, known as beam fanning, results from the nonuniform amplification of the scattered beams (at the expense of the input beam) along a preferential direction that is determined by the direction of input beam with respect to the c-axis of the photorefractive crystal. A semilinear oscillator can be constructed by placing a reflector along the direction where the beam fanning prevails. Under appropriate conditions, the reflector can be replaced by a fiber facet. A small amount of light reflected from the fiber can enhance selected sets of the fan gratings and initiate the oscillation. As the oscillation builds up, the fanning pattern collapses into an oscillation mode of the resonator defined by the fiber, and the light transmitted through the fiber increases from an initial value to a much higher steady-state value. When the

entrance face of the fiber is displaced or tilted (within a certain range) to a new location (or orientation), the transmitted optical power drops abruptly. However, after a certain characteristic time (on the order of a few seconds to a few minutes, depending on the experimental condition) new gratings are formed (as the old ones are erased) and the transmitted optical power recovers to the steady-state value. In this novel approach, the coupling of light from the laser to the fiber is adaptive and fault-tolerant. Although the optical feedback required for the oscillation can be provided by Fresnel reflection from either the entrance facet or the exit facet of the fiber or from the appropriate Bragg grating recorded in the core of the fiber, only reflection from the exit facet or from the Bragg grating recorded in the core of the fiber can automatically fulfill the mode matching condition. In both cases, the reflectivity needs to be optimized to achieve maximum coupling efficiency. In this program, for the first time we have successfully demonstrated a fault-tolerant (or self-tracking) laser-to-fiber coupler based on the a photorefractive semi-linear resonator.

1.2.3 Multimode-to-Singlemode Fiber Optic Coupler Based on Photorefractive Mutually-Pumped Phase Conjugation

When two laser beams (of the same color, but mutually incoherent) with appropriate wavelengths and polarizations enter a photorefractive crystal at proper angles, a set of gratings is generated by each incident beam via interference with its own scattered components. Under appropriate conditions, the set of gratings that is self-enhanced is the one that transforms each beam into the phase conjugate of the other. Such a phenomenon or process is know as mutually-pumped phase-conjugation (MPPC). The MPPC described above can thus transform the wavefront of a multimode beam (from a multimode fiber) to match that of a single mode beam and couple it efficiently into a single mode fiber. When the fibers are slightly misaligned from the optimum position/orientation, a new set of gratings that correct for the changes is self-generated, provided that the two beams remain intersecting (or overlapping) inside the crystal. The key material parameters that dictate the performance of the device are the coupling constant, the absorption coefficient, and the response time. All three parameters are fairly sensitive to wavelength. For a given material, and at an appropriate wavelength, the coupling efficiency and the degree of fault-tolerance can be maximized by a proper selection of the experimental configuration and the power ratio of the two input beams. A highly efficient and stable multimode-to-singlemode fiber optic coupler with performance parameters (i.e., coupling efficiency and degree of fault-tolerance) one to two orders of magnitude better than any other conventional techniques know to date was successfully developed under this program.

1.3 Progress and Accomplishments

Areas of significant progress and major accomplishments in our study of energy coupling and spatial mode conversion in photorefractive waveguides, fibers and bulks for applications in laser-to-fiber coupling include:

1. Fabrication and acquisition of several c-axis photorefractive waveguide and fiber samples including, a thin plate of strontium barium niobate (SBN), a SBN wedge, a copper doped barium strontium potassium sodium niobate (BSKNN:Cu) wedge, a SBN fiber, and an iron doped lithium niobate ($LNbO_3$:Fe) fiber.

2. Characterization of the photorefractive properties of various samples.

3. Experimental demonstration of energy transfer from free propagating beam to guided beam in planar waveguides and wedges.

4. Experimental demonstration of energy transfer among different guided beams in planar waveguides and wedges.

5. Theoretical result for energy transfer from higher order to lower order modes for the case of 10 guided-modes.

6. Identification of photorefractive core/cladding fiber configurations which enhance mode conversion and minimize energy loss.

7. The first experimental demonstration of fault-tolerant laser-to-fiber coupling.

8. The first experimental demonstration of an efficient and fault-tolerant multimode to singlemode fiber optic coupler.

1.4 Publications and Presentations

A. Chiou, P. Yeh, and C. Gu, "Spatial mode conversion in photorefractive fibers", in OSA Annual Meeting Technical Digest, 1993 (Optical Society of America, Washington, D.C., 1993), Vol. 16, pp.7

A. Chiou, P. Yeh, C. Gu, and R. Neurgaonkar, "Beam coupling and spatial mode conversion in photorefractive planar waveguide", IEEE LEOS '93 Conference Proceedings, San Jose, CA, November 1993, pp.319.

A. Chiou, P. Yeh, C.-X. Yang and C. Gu, "Photorefractive resonators for fault-tolerant coupling", OSA 1994 Annual Meeting, Dallas, TX, October 1994.

A. Chiou, P. Yeh, C.-X. Yang and C. Gu, "Photorefractive resonators for adaptive fault-tolerant coupling", SPIE's Newsletter, Optical Processing and Computing Technical Working Group, Vol. 5, No. 2, 2, November 1994.

A. Chiou, P. Yeh, C.-X. Yang and C. Gu, "Photorefractive coupler for fault-tolerant coupling", to appear in *Photonics Tech. Lett.* July 1995.

A. Chiou, P. Yeh and C. Gu, "A photorefractive spatial mode converter for multimode to singlemode fiber-optic coupling", to appear in *Opt. Lett.* May 1995.

A. Chiou, P. Yeh, C.-X. Yang and C. Gu, "Multimode to singlemode fiber-optic coupling using mutually-pumped phase conjugation", to be presented in Topical Meeting on Photorefractive Materials, Effects and Devices, June 1995, Colorado.

A. Chiou, "Spatial mode conversion in photorefractive waveguides, fibers, and bulk materials", invited paper, SPIE's 1995 International Symposium on Optics, Imaging, and Instrumentation, July, 1995, San Diego, CA.

1.5 Technical Disclosure

"Photorefractive Coherent Optical Funnel", Arthur Chiou and P. Yeh, Rockwell International Technical Disclosure No. 93SC048.

"Photorefractive Mode Converter For Coupling of Laser Light From a Multimode Fiber to a Single Mode Fiber", Arthur Chiou and P. Yeh, Rockwell International Technical Disclosure No. 94SC107.

2.0 Technical Discussion

This program focuses on the study of photorefractive dynamic holograms for applications in optical links involving lasers, waveguides, and fibers. The objective of the program is to demonstrate and develop novel techniques for efficient coupling of laser light into singlemode fibers with a large degree of fault-tolerance. Efficient and fault-tolerant laser-to-fiber or fiber-to-fiber couplers are critical components in fiber optical communication networks. In this section, we briefly introduce the photorefractive effect and discuss some selected photorefractive phenomena and devices studied under this program for fiber optics coupling applications.

2.1 A Brief Introduction to Photorefraction

Literally, photorefraction means light-induced change of refractive index. Conventionally, however, the photorefractive effect[1,2,3] refers to the spatial modulation in refractive index in electrooptic crystal under nonuniform illumination of light which is usually caused by the interference of two or more mutually-coherent optical beams inside the crystal. Since the spatial modulation of refractive index inside a volume is essentially a volume phase hologram, almost all the photorefractive phenomena involve the diffraction of light by the dynamic holograms generated by the interference of the optical beams inside the crystal. According to a widely accepted physical model of photorefraction,[4,5] the index modulation (or phase holograms) is generated by the following processes: 1) photoionization of charge carriers (electrons and/or holes) in the bright regions (or fringes) from some impurity levels to the conduction or valence band; 2) migration of free carriers due to diffusion and/or drift; 3) retrapping of the charge carriers in the dark regions by some trap centers; 4) formation of nonuniform charge distribution and the associated nonuniform space charge field as prescribed by Poisson equation; 5) modulation of the refractive index (or equivalently, the formation of phase holograms) by the space charge field via the linear electrooptic (Pockel) effect.

Some of the most popular photorefractive materials[6–9] that have been studied to date include barium titanate ($BaTiO_3$), potassium niobate ($KNbO_3$), lithium niobate ($LiNbO_3$), lithium tantalate ($LiTaO_3$), strontium barium niobate ($Sr_{1-x}Ba_xNb_2O_6$ or SBN) barium strontium potassium sodium niobate ($Ba_{1-x}Sr_xK_{1-y}Na_yNb_5O_{15}$ or BSKNN), bismuth silicon oxide ($Bi_{12}SiO_{20}$ or BSO), bismith gemanium oxide ($Bi_{12}GeO_{20}$ or BGO), gallium arsinide (GaAs), Indium phosphite (InP), Gallium phosphite (GaP), and cadmium telluride (CdTe). The

approximate range of wavelength in which the photorefractive effect is significant is illustrated in Fig. 1 for some selected materials.

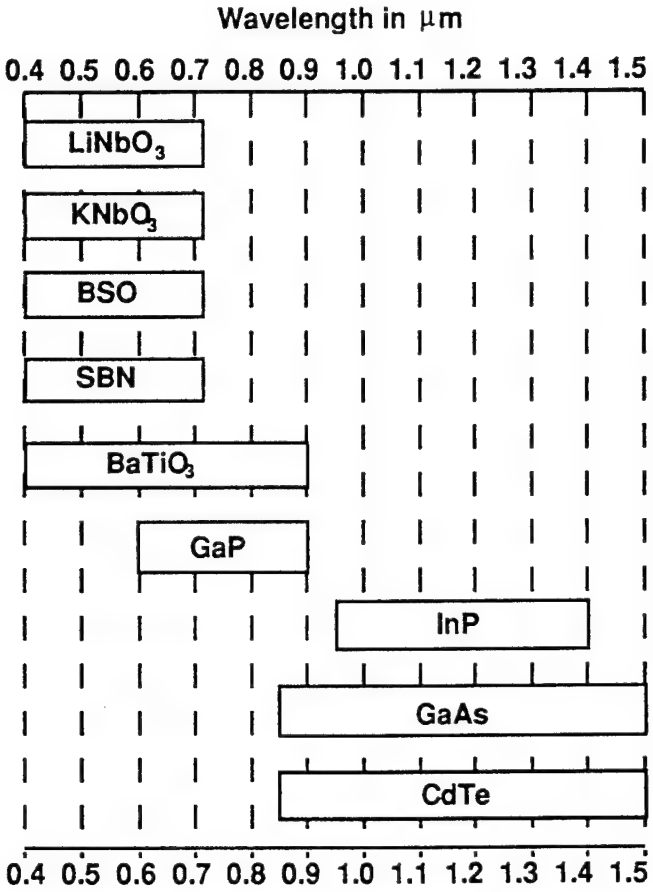

Fig. 1 Approximate spectral range of some selected photorefractive materials.

A selected number of photorefractive phenomena that are closely related to the novel device concepts developed under in this program for fiber-optic coupling applications are outlined below.

2.2 Photorefractive Two-wave Mixing

Photorefractive two-wave mixing[5,10] (also known as two-beam coupling, or energy coupling) refers to the nonreciprocal energy transfer from one optical beam to another mutually coherent beam when the two interact inside a photorefractive crystal. The net result is the amplification of one beam (usually referred to as the signal beam) at the expense of the other (usually referred to as the pumping beam). This unique property is a direct consequence of the nonzero spatial phase shift between the index grating and the interference fringes. For a given

index modulation, the energy transfer is maximum when the phase shift is $\pi/2$. The $\pi/2$ phase shift occurs naturally when diffusion is the dominant charge transport mechanism. Qualitatively, the process [i.e., energy gain (loss) in the signal (pumping) beam] can be explained by the self-diffraction of pumping (signal) beam by the adaptive volume hologram written by the two beams in conjunction with the constructive (destructive) interference of the diffracted component of one beam with the transmitted component of the other (Fig. 2).

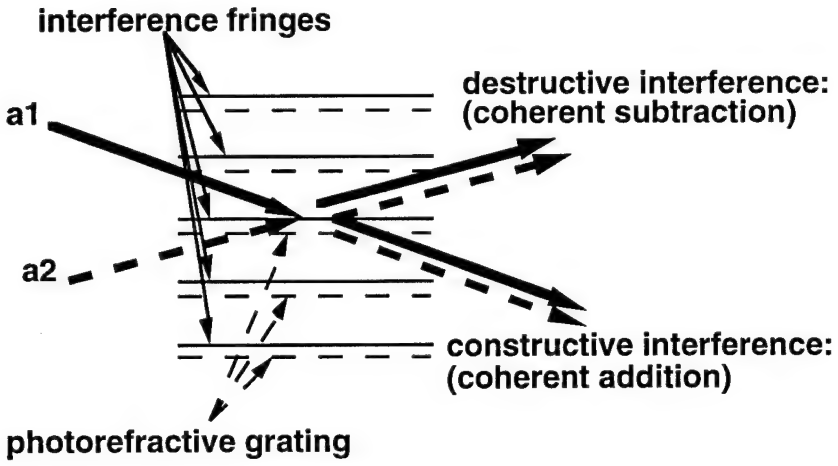

Fig. 2 A qualitative explanation of enrage transfer in photorefractive two-beam coupling in terms of the constructive (or destructive) interference of the transmitted and the diffractive components of two interacting beams.

Although energy coupling in photorefractive bulk crystals has been studied extensively and demonstrated for many application concepts, including coherent image amplification,[11–14] image processing,[15–22] and optical interconnections,[23–29] the study of such an effect in guided wave structures has attracted much less attention,[30–34] mainly because photorefractive waveguides or fibers have not been readily available to most of the researchers. During the first phase of this program, we have investigated the potential applications of photorefractive waveguides and fibers for the conversion and coupling of a free propagating laser beam to low-order guided modes in appropriate waveguide structures.[35,36] Spatial mode conversion in photorefractive waveguide structures can be viewed as a natural extension of two-wave mixing in bulk materials. As an example, consider a multimode waveguide or fiber that can support many guided modes. Geometrically, a higher order mode can be represented by a wave-vector $\mathbf{K}_2$ propagating at an angle θ_2 (relative to the fiber axis) which is larger than the corresponding angle θ_1 associated with a lower order mode (Fig. 3a). If the fiber is made of photorefractive material with c-axis parallel to the fiber axis, energy can be transferred from the higher order to the lower order modes via

photorefractive beam coupling as the optical wave propagates towards the "+c" direction (Fig. 3b). In principle, if the product of the coupling constant and the interaction length (ΓL) is sufficiently large (and assuming negligible loss), all the energy will eventually be transferred to the lowest order mode. In addition, the dynamic nature of the photorefractive grating can adaptively correct for certain changes in the input beam geometries such as the direction of beam injection and the beam profile. This process can therefore facilitate the coupling of a laser beam to a fiber or waveguide by not only improving the coupling efficiency but also reducing the sensitivity to misalignment.

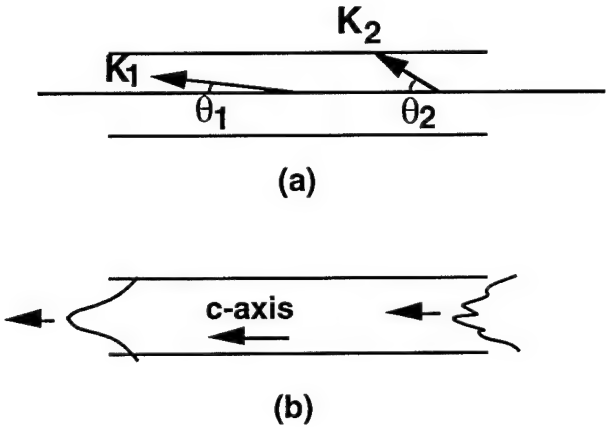

Fig. 3 (a) Geometrical representation of wave-vectors associated with higher order and lower order modes in a multimode waveguide; (b) a conceptual illustration of spatial mode conversion in a c-axis oriented photorefractive waveguide.

A form of spatial mode conversion related to the one described above was first observed in $BaTiO_3$ slab waveguides in 1989[34] (as funneling and antifunneling of light). In a later year, the same research group reported the observation of similar phenomena (of self-focusing/defocusing) in photorefractive bulk crystal.[37] A closely related phenomenon of self-trapping of an optical beam in photorefractive material (i.e., the existence of photorefractive spatial solitons) has also been predicted theoretically[38] and observed experimentally.[39] However, the effects observed were extremely weak compared with the typical two-beam coupling in bulk crystal. In this program, we focus on the enhancement of these effects and on the harnessing of these phenomena for the improvement of coupling efficiency and fault-tolerance in coupling light from a laser source to a fiber or waveguide. Progress in this area is summarized in Section 3.1.

2.3 Photorefractive Phase Conjugate Resonator

When a laser beam with an appropriate wavelength and polarization enters a photorefractive crystal, the intensity distribution of the beam at the exit face of the crystal usually exhibits a characteristic fan shape. Such a phenomenon, known as beam fanning,[40] results from the nonuniform amplification of the scattered beams (at the expense of the input beam) along a preferential direction that is determined by the direction of input beam with respect to the c-axis of the photorefractive crystal. With a few exceptions (such as power limiter,[41,42] novelty filter,[17,43] and the phase conjugate resonator described below) where this effect is used constructively, beam fanning normally degrades the signal-to-noise ratio, and is considered a nuisance in most of the imaging applications. Techniques[44–46] to reduce the beam fanning effect have been reported in the literature, and this issue remains a subject of important research to date.

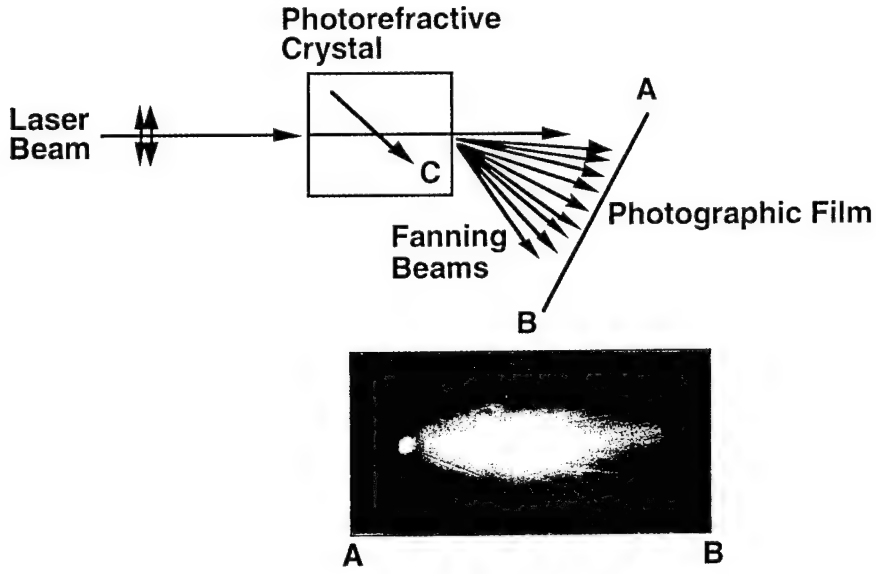

Fig. 4 An illustration of beam fanning effect in a barium titanate sample.

A fascinating application of the beam fanning effect described above is the construction of a phase conjugate optical resonator. A semilinear (or a linear) resonator can be constructed by placing one (or two) reflector(s) along the direction where the beam fanning prevails as shown in Fig. 5.[47–49] Under appropriate conditions where the optical gain associated with one or more modes of the optical cavity exceeds the loss, optical power in these modes can build up by extracting the energy from the injecting (or pumping) beam, and oscillation of the modes can be observed. For the case of a linear resonator, the cavity is defined by the two external reflectors; whereas for the semilinear resonator, it is formed by the photorefractive crystal in one end, and the

external reflector in the other. As the oscillation builds up, a phase conjugate[50–52] replica of the pumping beam is generated by a process known as photorefractive four-wave mixing,[1–3] hence the name phase-conjugate resonator. The idea of using a semilinear passive phase conjugate resonator for laser-to-fiber coupling was first proposed and analyzed by Schuenke in 1987.[53] However, no experimental evidence has ever been reported to date. The lack of experimental demonstration is probably because the optical gain achieved in most crystals (and in most of the experimental configurations) is simply not high enough to compensate for the cavity loss, which is enormous in this case due to the very small size of the fiber facet. Although Photorefractive SPCR and some related devices in a variety of configurations were reported in the early 1980s, experimental investigations of SPCR involving small aperture (on the order of 1 mm or less) was not reported until 1993. Independent of our experimental investigation carried out in this program, a group of researchers from Australia reported some interesting experimental results from a different context. In their work,[54] a plastic transparency (which had a transmission of about 94%) with a 1 mm diameter hole and a focusing lens were inserted into a cavity consisting of a barium titanate crystal at one end and a 90% plane reflector at the other end. Such an arrangement allows the cavity to resonate only in its lowest order mode when light from the output of a multimode fiber was injected into the crystal at an appropriate angle. Although the result was interpreted as the efficient conversion of multimode fields into single spatial mode, no data on the coupling of the single spatial mode beam into a single mode fiber were reported.

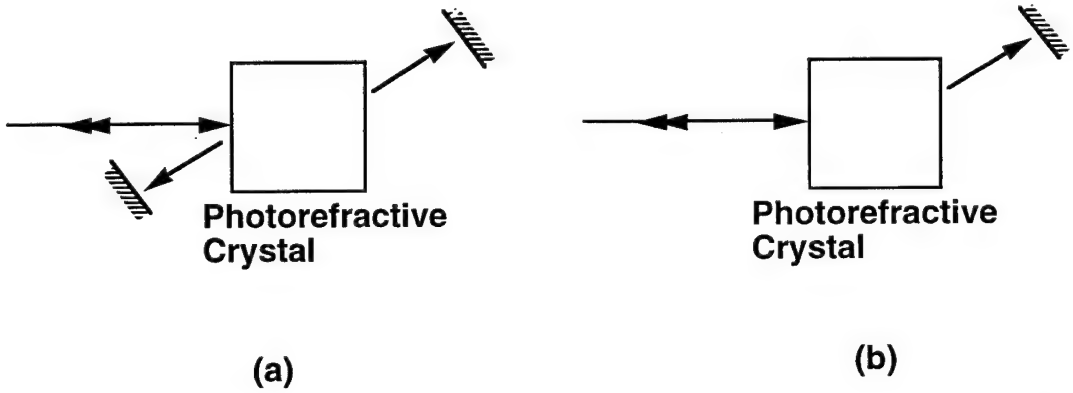

Fig. 5 A schematic illustration of a (a) linear phase conjugate resonator (LPCR), and (b) semilinear phase conjugate resonator (SPCR).

During the course of this program, we have successfully demonstrated, for the first time, a fault-tolerant laser-to-fiber coupler which is based on a photorefractive semilinear resonator with the fiber facet as a partial reflector. We have shown that a small amount of light reflected back from

the fiber can enhance selected sets of the fan gratings to initiate and sustain the oscillation. As the oscillation builds up from the feedback into the noise grating, the fanning pattern collapses into an oscillation mode of the resonator defined by the fiber facet, and a phase conjugate signal of the input beam increases from zero to a steady-state value while the light transmitted through the fiber also increases from an initial value to a much higher steady-state value. When the end of the fiber is displaced or tilted (within a certain range) to a new location (or orientation), both the phase conjugate and the transmitted signals drop abruptly. However, after a certain characteristic time (on the order of a few seconds to a few minutes, depending on the experimental condition) new gratings are formed (as the old ones are erased) and both signals recover to their steady-state values. In this novel approach, the coupling of light from the laser to the fiber is therefore adaptive and fault-tolerant.

2.4 Mutually Pumped Phase Conjugation (MPPC)

When two laser beams are injected at appropriate geometry[55–57] into certain photorefractive crystals such as SBN or $BaTiO_3$, they can together write and share a common set of gratings such that the readout of the gratings by each beam represents the phase conjugate replica of the other. Such a phenomenon, which is known as mutually pumped phase conjugation, is illustrated schematically in Fig. 6. In general, the output A3 (or A4) represents the phase conjugate replica of the spatial wavefront of A1 (or A2), whereas the temporal signature of A3 (or A4) is the same as A2 (or A1). In other words, MPPC is unique in that it phase conjugates the spatial information of each input beam back to the port where each beam originates, but transmits the temporal signal of each input to the other port. The two beams can carry different spatial images and can be either of the same nominal wavelength (from two separate laser sources) or even of different wavelengths depending on the geometry. The latter is referred to as the Double Color Phase Conjugator (DCPC).[58]

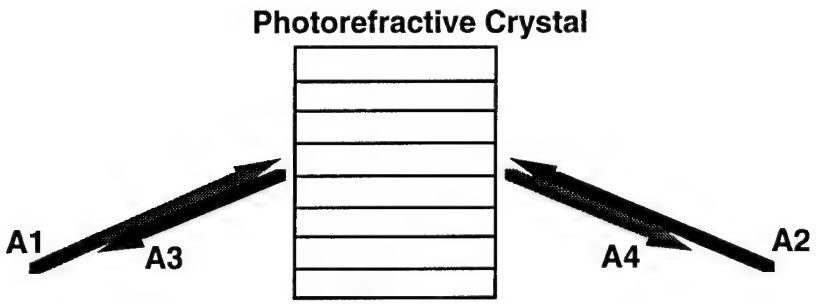

Fig. 6 A schematic illustration of mutually-pumped phase conjugation (MPPC).

One of the most important potential applications of mutually pumped phase conjugation (or MPPC), which has been studied extensively, is in optical interconnections that link a set of transmitting channels to another set of receiving channels.[59–62] In a typical scenario, the signal carrying beam in each channel is transmitted through a fiber which can be either singlemode or multimode. Under this program, we have shown that MPPC is capable of transforming the spatial wavefront of a multimode beam (designated the signal beam in Fig. 7) to match that of a singlemode beam (designated the beacon beam in Fig. 7) and coupling it efficiently into a SMF. In addition to the very high efficiency, optical links based on MPPC have a unique advantage (compared with other conventional approaches) in that it is extremely insensitive to misalignment. When the fibers are displaced from the optimum position/orientation, a new set of gratings that corrects for the changes is self-generated provided that the two beams remain intersecting (or overlapping) inside the crystal. As a result of this self-healing process, the technique can tolerate a large amount of angular and lateral misalignments. In sharp contrast, conventional techniques using single- or multiple- lens system for multimode to singlemode coupling are so sensitive to both angular and lateral alignment that it is extremely difficult to align the system and hold the coupling efficiency at a steady and significant level. Although many features of MMPC of two or more Gaussian beams and optical fibers in a wide variety of configurations and context have been studied and reported,[59– 62] to the best of our knowledge, our experimental results represent the first demonstration of its application for efficient and fault-tolerant multimode to singlemode fiber-optic coupling.

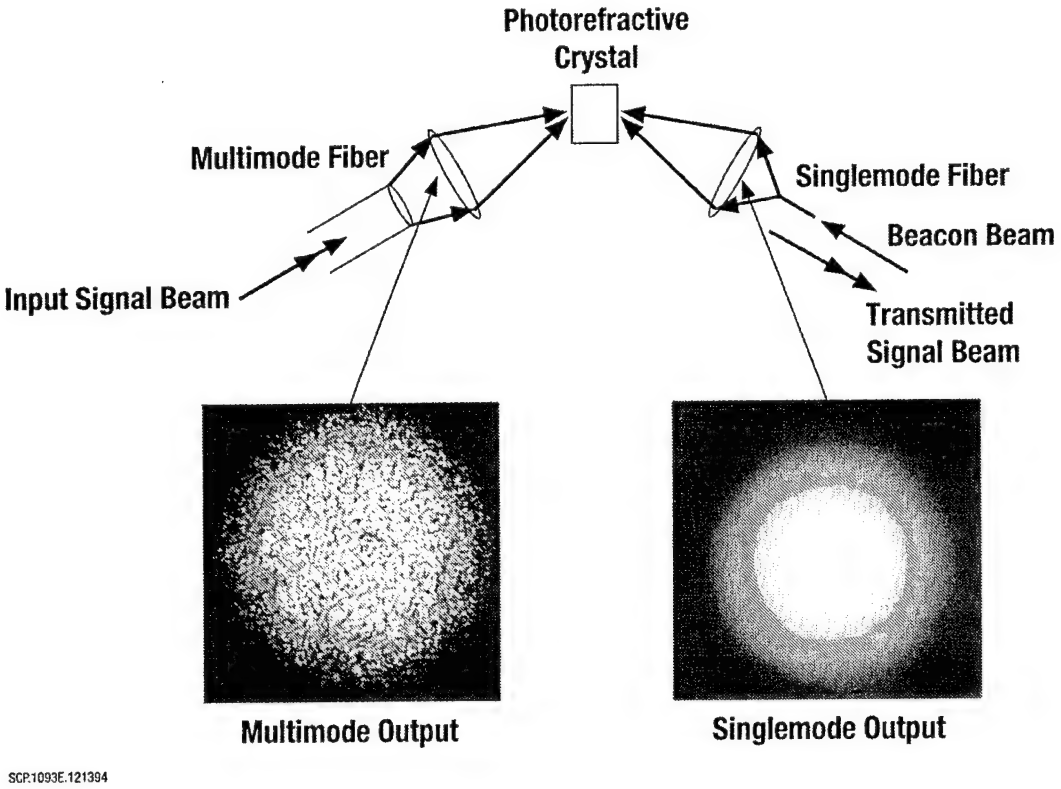

Fig. 7 A schematic illustration of the spatial mode conversion and efficient coupling of the output of a multimode fiber into a single mode fiber.

The physical mechanism responsible for the mutually pump phase conjugator (MPPC)[59] is closely related (but not identical) to the optical oscillation in SLPR used for fault-tolerant laser-to-fiber coupling discussed in the previous section. From the practical point of view, the key difference lies in the fact that one or more beacon beams originated from other channel(s) are always required in the case of MPPC; whereas in the case of laser-to-fiber coupling based on SPCR, no beacon beam is required form the other end, since it is self-generated by reflection of the signal beam at the fiber facet.

3.0 Progress

During the early phase (the first year) of this program, we focused on the potential applications of spatial mode conversion in photorefractive waveguides and fibers for laser to fiber coupling. Our theoretical investigations began with a simple model to analyze some of the key features in spatial mode conversion. Specifically, we have used plane-wave approximation to analyze 1) the dependence of coupling constant on the difference of the effective mode indices, 2) energy coupling between "N" modes for the case of N = 10, assuming uniform coupling constant, and 3) energy coupling of two modes in photorefractive fibers with core/cladding structure. The theoretical results indicate that a low-loss core with a photorefractive cladding is preferable (in comparison with other geometries) because it potentially converts the higher orders into lower order modes efficiently with minimum loss due to absorption and/or scattering. Unfortunately, no such samples are available to date.

Experimentally, we have studied beam coupling and spatial mode conversion in SBN Plates wedges; and fibers, and also in lithium niobate fibers. Even though beam coupling and spatial mode conversion can be observed and measured in most of our samples, they are too weak to be of any practical values. Our progress in photorefractive waveguides and fibers for fault-tolerant laser-to-fiber coupling was reported in two conference papers and documented in the First Annual Technical Report (Report #71074.AR) of this program.

Faced with limited success in the applications of photorefractive waveguides and fibers and the lack of availability of suitable samples at the end of the first year, we proposed to redirect our technical efforts towards the use of photorefractive crystalline bulks in conjunction with conventional glass fibers. Following the approval of our proposed effort by our technical monitor, we began to investigate the potential applications of phase conjugate resonators and mutually pumped phase conjugation for laser-to-fiber and fiber-to-fiber couplings in the second part of this program. Although the ultimate wavelengths of interest are in the proximity of the 1.3 μm and 1.5 μm (from semiconductor laser sources), we chose to start our feasibility study at 514.5 nm using an argon ion laser because photorefractive crystals such as barium titanate and strontium barium niobate, which exhibit strong phase conjugation at this wavelength (without requiring any external applied field), are readily available. Progress in these efforts and technical issues associated with the applications of these novel techniques using semiconductor lasers in wavelengths of particular interest to the fiber optic communication industry (i.e., 1.3 μm and 1.5 μm) are discussed in the following sections.

3.1 Laser-to-Fiber Coupling Using A Semilinear Phase Conjugate Resonator (SPCR)

In Section 2.3, we discussed the principle of operation of using a semilinear passive phase conjugate resonator (SLPR) for laser-to-fiber coupling. The experimental configurations and results are discussed in greater detail below in this section.

In our experimental demonstration, we selected a 45°-cut barium titanate crystal with very strong beam fanning surrounding the c-axis direction. Because of the relatively large coupling coefficient associated with this crystal in the 45° geometry, we anticipated that self-starting and sustaining oscillation should be achievable with relatively small (on the order of 1mm or less) reflector. In our first attempt, we used a variable aperture and a beam splitter (R = 50%) to access the minimum size of the reflector required and to find the optimum geometry (Fig. 8). As the oscillation built up form the noise grating, a phase conjugate signal (as monitored by the detector D2 in Fig. 8) appeared; and along with the light transmitted through the aperture and the partial reflector (monitored by the detector D1 in Fig. 8), both signals increased to their steady state values. Self-starting and stable oscillation were achieved for aperture diameter as small as 800 μm. The optimum geometry was determined by varying the angular and linear positions of the crystal and the reflector-aperture assembly to maximize the steady state value of the transmitted optical power. By detuning the reflector-aperture assembly from its optimum position, we verified that such a configuration is relatively insensitive to linear and angular misalignment. The self-healing (self-tracking) capability of the resonator was clearly demonstrated by observing the sharp drop of both the phase conjugate and the output signals when the reflector was detuned from its optimum position and the self-recovery of the signals to their original level. A typical experimental result for the case when the reflector was rotated by about 1° around the vertical axis was depicted in Fig. 9. A plot of the coupling efficiency (defined as the transmitted optical power at the steady state/optical power injected into the photorefractive crystal) as a function of the relative orientation of the partial reflector (as displayed in Fig. 10) revealed that sustained and stable oscillation with coupling efficiency > 15% was achieved for angular misalignment of about ± 1.5°. The corresponding amplification factor (defined as the transmitted optical power monitored by the detector D1 at steady state oscillation/that without oscillation) was also shown in Fig. 9.

We observed that the SLPCR is more sensitive to the vertical misalignment than to the horizontal. Such a behavior is anticipated because the beam fanning effect, which is preferentially

in the horizontal plane, cannot accommodate the beam walk-off along the vertical direction as efficiently as it does in the horizontal plane.

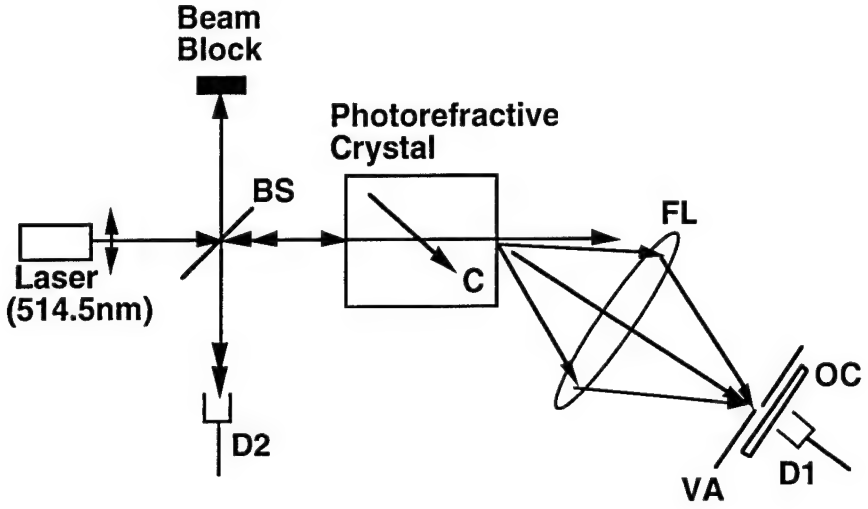

Fig. 8 Experimental configuration of a semilinear phase conjugate resonator (SPCR) using a 50% beam splitter and a variable aperture as the output coupler. BS: beam splitter, FL: focusing lens, OC: output coupler, VA: variable aperture, D: detector.

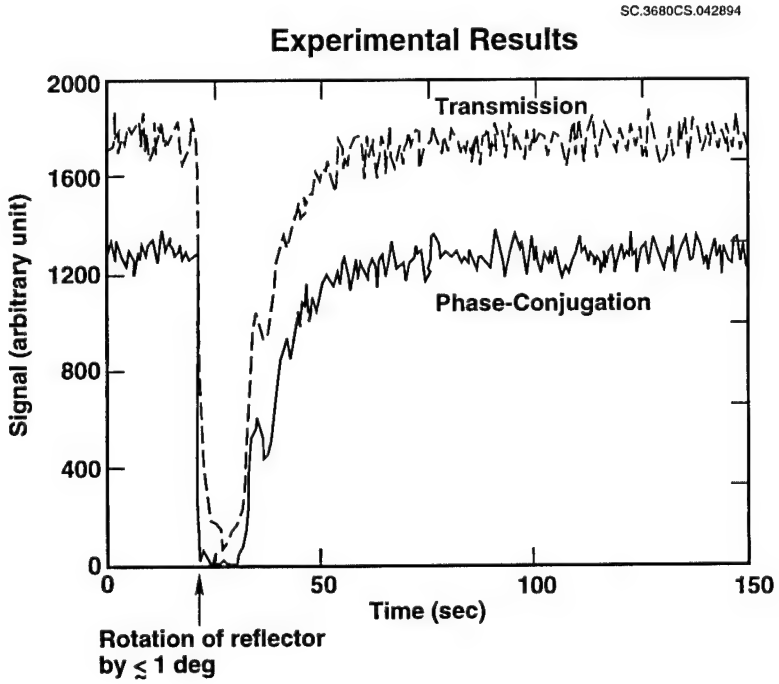

Fig. 9 Experimental results showing the decay and the self-recovery of the oscillation in SPCR (see Fig. 8) when the output coupler was rotated (by about 1° along the vertical axis) from the optimum position. The top and the bottom traces represent the transmitted and the phase conjugate signals, respectively.

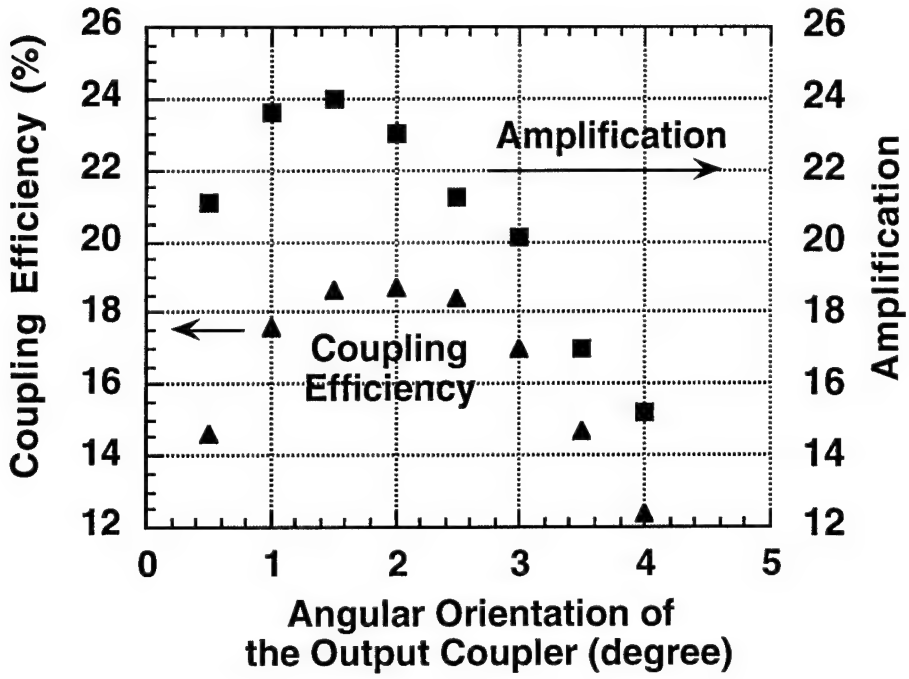

Fig. 10 The coupling efficiency (▲) and the amplification factors (■) of the SPCR as a function of the verticular angular position of the output coupler.

In the second set of experiments, we used various sizes of circular chromium reflectors (ranging from 400 μm to 20 μm) deposited on glass substrate as the reflector. Self-starting and stable oscillation was observed with chromium disk diameter as small as 40 μm. The distinct intensity distributions behind the glass substrate before the oscillation started and after the oscillation buildup to a steady state were compared in Fig. 11. for the case of a 40 μm diameter chromium reflector. Following these encouraging results, we began our third set of experiments in which the chromium reflectors were replaced by a polished facet of an optical fiber.

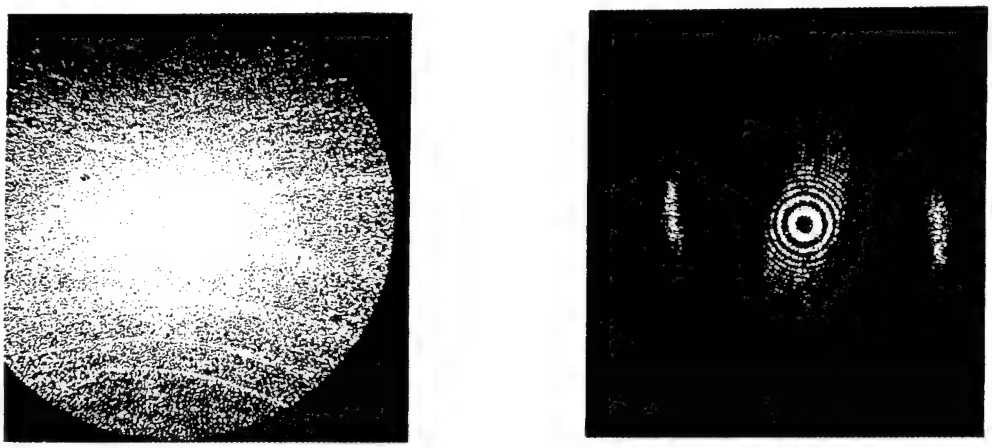

(a) Without Oscillation (b) With Oscillation

Fig. 11 Intensity distribution at the output of SPCR using a 40 μm diameter chromium circular disk on glass as the output coupler (a) prior to oscillation buildup, (b) when the oscillation reaches a steady state.

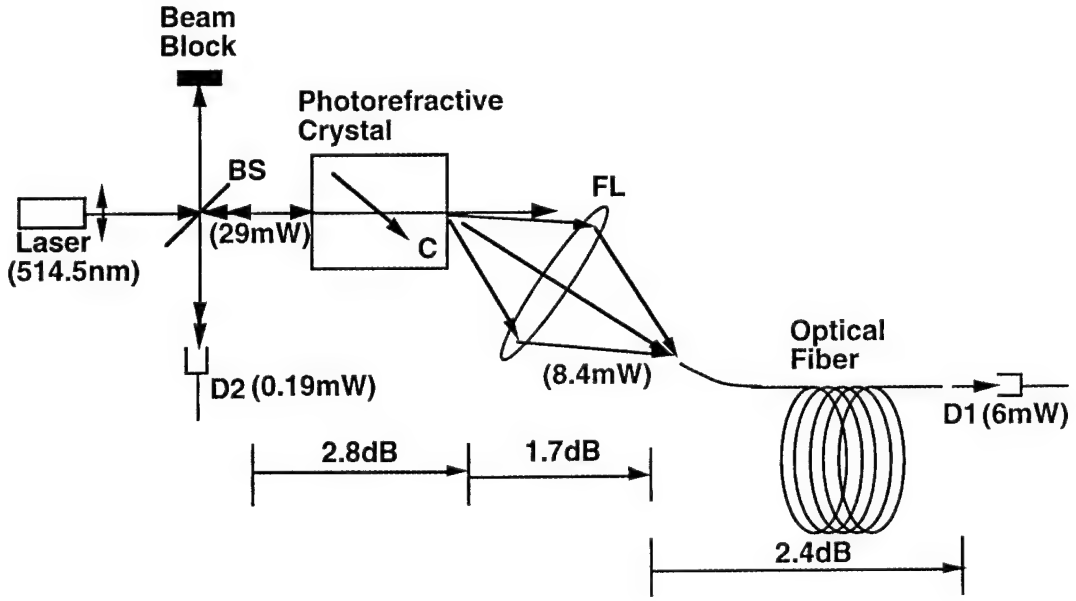

Fig. 12 Experimental configuration for fault-tolerant laser-to-fiber coupling using SPCR.

The experimental configuration is illustrated schematically in Fig. 12. The output from an argon ion laser (514.5 nm, and with horizontal polarization) was injected into a 45°-cut barium titanate crystal (5.6 mm × 5.5 mm × 5.9 mm) with an angle of incidence of about 11°. The transmitted beam fanned preferentially along the direction of the c-axis as shown in the figure. The

fanning beams were loosely focused by a focusing lens (FL, focal length = 38 mm, diameter = 50 mm) to one facet of a glass fiber (core diameter = 400 μm, cladding diameter = 500 μm, numerical aperture = 0.16, length = 4 m) mounted on a gimbal mount (not shown in the figure) so that its position/orientation can be adjusted in five degrees of freedom. The orientation of the entrance face of the fiber was adjusted manually so that the reflected light approximately retraced its incoming path back to the crystal. To provide sufficient optical feedback to assist the initiation of the oscillation, the end face of the fiber was polished and coated with thin alternating layers of TiO_2 and SiO_2 so that the Fresnel reflection at 514.5 nm was about 36%. A beam splitter BS was placed in the front end of the crystal to sample the phase conjugate beam for monitoring by a detector D2. At the exit face of the fiber, the transmitted optical power was monitored by another detector D1.

In the initial state, when the input beam (~29 mW) was first injected into the crystal, it began to fan towards the focusing lens, and the light coupling efficiency through the fiber was relatively low (about a few percent, depending on the exact location and orientation of the entrance face of the fiber). During this period, no phase conjugate signal was detected. After a period ranging from a few seconds to a few minutes (depending on the experimental condition), as some selected sets of fanning gratings were gradually enhanced by the reflected light and its diffracted components, both the phase conjugate and the transmitted signals increased to some steady state values. A small change in either the position or the orientation of the entrance face of the fiber resulted in an abrupt drop of both signals followed by a slow recovery of both back to their steady state values. An example of the transmitted and the phase conjugate signals (upper trace for output from detector D1 and lower trace for that from D2) at the steady state and as the entrance face for the fiber was displaced transversely first by 250 μm, and then followed by another 250 μm, was shown in Fig. 13. Note that the total displacement was larger than the diameter of the fiber core, which is 400 μm. In addition to linear displacement, we changed the orientation of the fiber facet (or the crystal) by a few degrees and verified that the system is also insensitive to angular misalignment.

Experimental Result on Fault-Tolerance

Upper Trace: Optical Power Transmitted Through the Fiber Sample
Lower Trace: Optical Power of Phase Conjugate Reflection

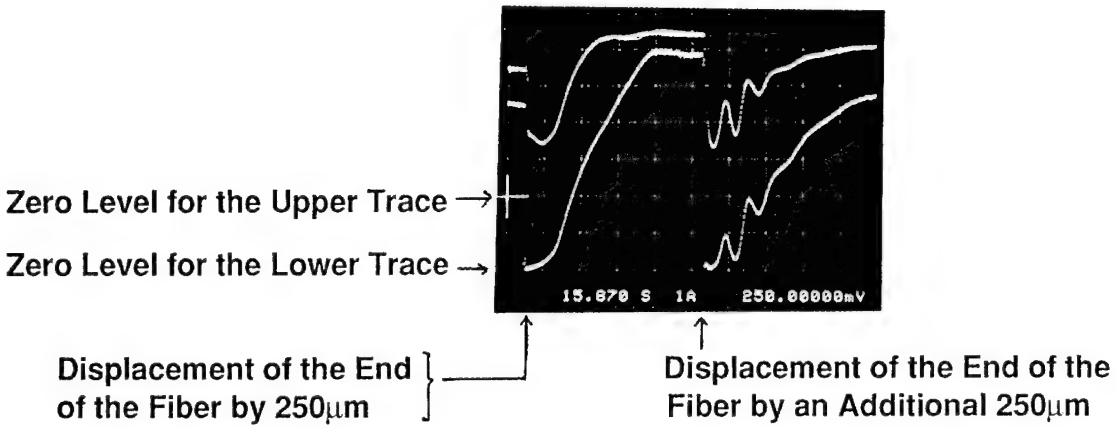

Fig. 13 Experimental results showing fault-tolerant coupling. The upper and the lower traces correspond to output signals from detectors D1 and D2, (i.e., the transmitted and the phase conjugate signals), respectively.

In this experiment, the coupling efficiency (measured by the optical power output transmitted through the fiber divided by that at the entrance face of the fiber) at the steady state was about 58% and the corresponding phase conjugate reflectivity (defined by the ratio of the optical power of the phase conjugate beam to that of the input beam at the entrance face of the crystal) was about 1.3%. However, the net coupling efficiency (measured by the optical power output transmitted through the fiber divided by that injected into the crystal) was only 20%. Loss of optical power (in dB) in each stage is indicated in the lower part of Fig. 12. Key factors that contribute to the energy loss include the Fresnel reflection at the front and back faces of the crystal (~ 0.8 dB), absorption inside the crystal (~ 2.0 dB), incomplete pump depletion (~ 0.4 dB), energy loss at the focusing lens (~ 1.3 dB), and energy loss in coupling into the fiber (~ 2.4 dB). Of these factors, the Fresnel loss can be eliminated by antireflection coating the crystal faces; absorption inside the crystal can be reduced and pump depletion can be improved by proper selection (or doping and oxidation/reduction) of the crystal and/or operating at optimum wavelength; energy loss at the focusing lens can be reduced by using a lens with higher numerical aperture and/or a photorefractive crystal with smaller beam-fanning cone angle; and energy loss in coupling into the fiber can be reduced by optimizing the amount of light reflected back from the fiber. Although the optical feedback required for the oscillation can be provided by Fresnel reflection from either the entrance facet or the exit facet of the fiber or from the appropriate Bragg

grating recorded in the core of the fiber,[63–66] only reflection from the exit facet or from the Bragg grating recorded in the core of the fiber can automatically fulfill the mode matching condition. In both cases, the reflectivity needs to be optimized to achieve maximum coupling efficiency. Several techniques for preparing the fiber facet or core for optimum reflectance are shown in Fig. 14.

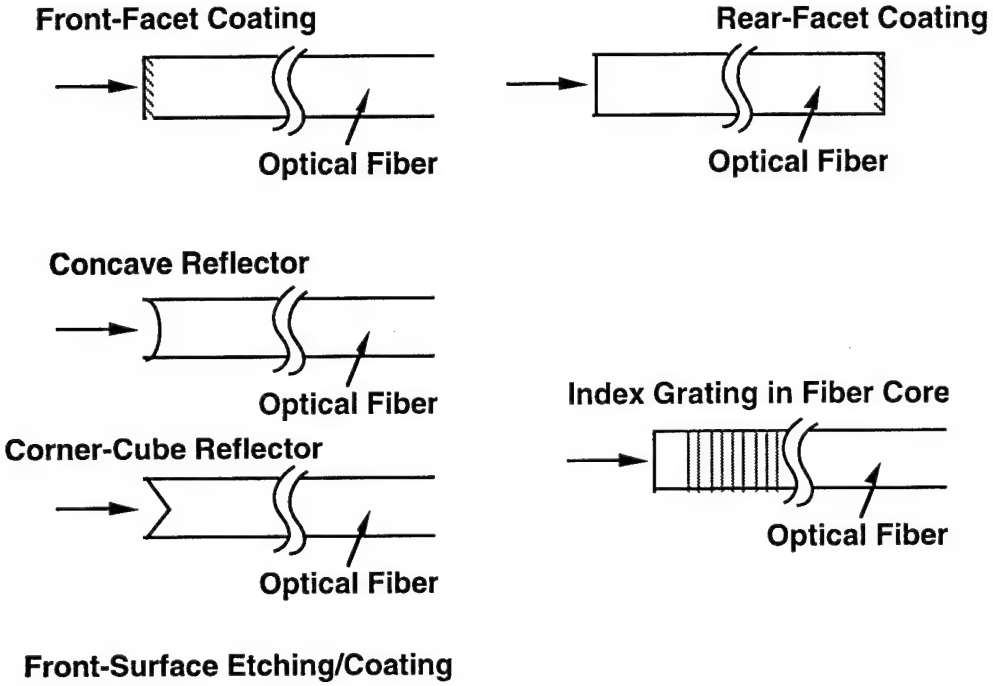

Fig. 14 Techniques for optimizing the optical feedback from the fiber to maximize the coupling efficiency.

In addition to the experimental investigations discussed above, we have studied a simple theoretical model of SPCR using plane wave approximation to estimate the reflectance of the output coupler required for sustained oscillation. Our theoretical result indicates that the minimum reflectance (R_{min}) of the output coupler required for oscillation depends on the coupling strength (ΓL) of the photorefractive crystal. The result, as shown in Fig. 15, also reveals that for a given ΓL and a given mirror reflectance $R > R_{min}$, there exist two solutions corresponding to the case with high transmission and weak phase conjugation, and vice versa.

As a concise summary of the status and the prospect of fault-tolerant laser-to-fiber coupling using SPCR, we have illustrated (in Fig. 16) the performance of this novel technique (as we have achieved to date) and our projection for possible improvement in the future in comparison with that of the conventional approach

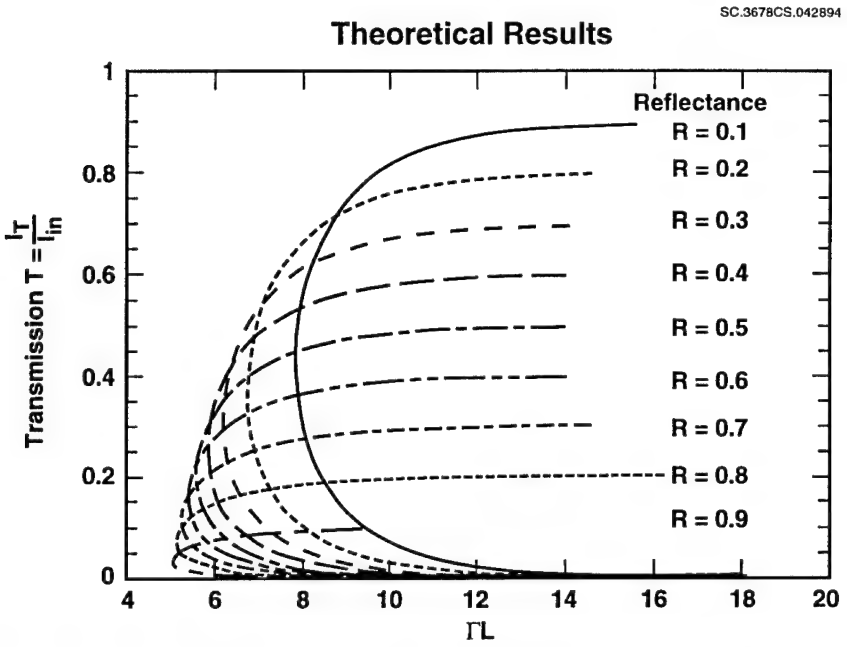

Fig. 15 Theoretical result showing the optical transmission of the SPCR as a function of the photorefractive coupling strength (ΓL) with the reflectance of the output coupler as a varying parameter.

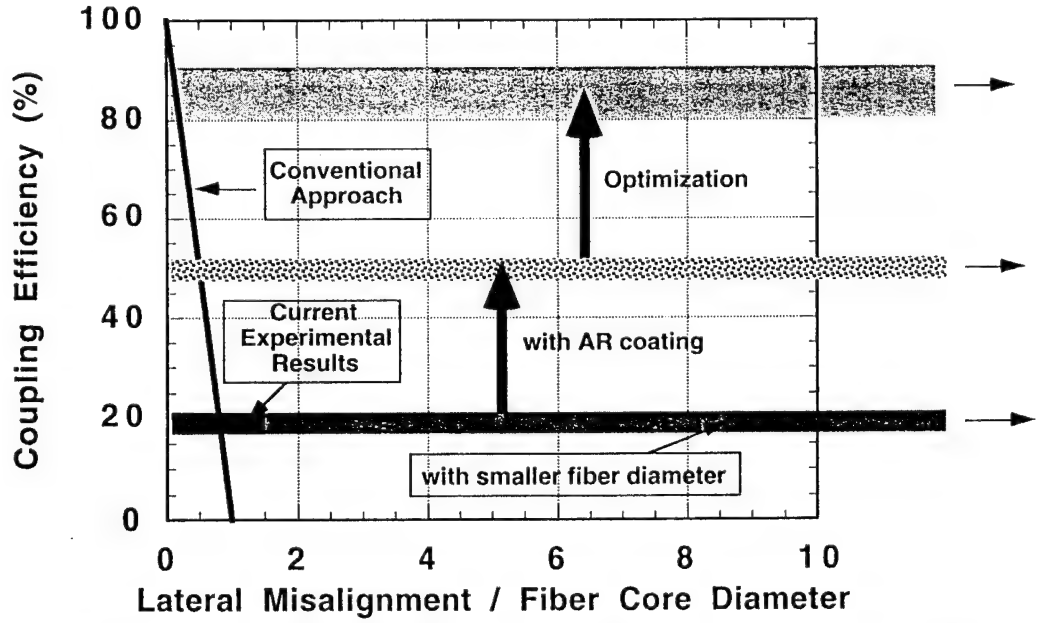

Fig. 16 A comparison of the current performance and the projected improved performance of SPCR to that of the conventional approach for laser-to-fiber coupling in terms of the coupling efficiency as a function of lateral misalignment (normalized to fiber core diameter).

3.2 A Photorefractive Spatial Mode Converter for Multimode to Singlemode Fiber Optic Coupling

Conventional techniques using a single- or multiple- lens system for coupling of light from a multimode fiber (MMF) to a singlemode fiber (SMF) suffer from two major technical difficulties. 1) The coupling efficiency is inherently low; the maximum coupling efficiency is fundamentally limited to 1/N where "N" is the number of spatial modes at the exit end of the multimode fiber, assuming that the energy is uniformly distributed among all the "N" modes. 2) The coupling efficiency is extremely sensitive to alignment. The mutually pumped phase conjugations, discussed in Section 2.4, are capable of coupling light from a MMF into a SMF with a coupling efficiency that can be several orders of magnitude higher than the "1/N" limit. In addition, due to its self-adaptive nature, tolerance to a fair amount of angular and/or lateral misalignments can be anticipated. In what follows, we describe the experimental details and results of our investigation.

The experimental configuration is illustrated schematically in Fig. 17. The output from an argon laser (514.5 nm) is split into two by a variable beam splitter, consisting of a half-wave plate ($\lambda/2$) and a polarizing beam splitter cube (PBS1). One of the beams (the beacon beam with horizontal polarization) is focused into a SMF (core diameter d = 2.9 μm, NA = 0.11, length = 10 m) via a microscope objective (MO1, 20x, NA = 0.40) and a five-axis SMF aligner/holder (FH1); while the other beam (the signal beam with vertical polarization) is focused into a MMF (core diameter D = 100 μm, numerical aperture NA = 0.37 length = 4 m) via another microscope objective (MO2, 10x, NA = 0.25). Using this arrangement, we typically achieve a coupling efficiency of about 60% for the SMF and 80% for the MMF. Although the signal beam injected into the MMF is vertically polarized, the polarization is severely scrambled by the MMF, rendering the output essentially unpolarized. A linear polarizer (P) is used to filter out the vertically-polarized component and transmit only the horizontal component, which is collected and focused by Lens L1 (focal length = 38mm, f/ = 0.7) into a 45°- cut barium titanate crystal (BT) as shown in Fig. 17. At the exit face of the crystal, the signal beam fans[4] strongly towards the c-axis (indicated by an arrow in Fig. 2) of the crystal. The fanning beam is collected and loosely focused by a second lens L2 (focal length = 38 mm, f/ = 0.7). The other end (facet) of the SMF (which is mounted on another five-axis fiber holder, FH2) is then placed approximately at the focal point of the multimode beam and oriented so that the two beams (signal and beacon) intersect inside the crystal. The interaction of the two beams inside the crystal generates a set of volume phase gratings that not

only efficiently (and adaptively) transforms the speckle pattern of the multimode output into the bell-shape intensity distribution of the SMF (see Fig. 7) but also directs the transformed beam into the SMF. Since the transformed beam is automatically mode-matched to that of the SMF (as a result of the phase conjugation process), the coupling efficiency (which is essentially limited by the diffraction efficiency of volume gratings responsible for the MPPC) can be very high. Two shutters (SH1 and SH2) are used to switched ON/OFF the two input beams; and two detectors (D1 and D2) are used to monitor the vertical and horizontal polarization components of the signal beam originated from the MMF, transmitted through the SMF and sampled by a polarizing beam splitter (PBS2) and a beam splitter (BS), respectively.

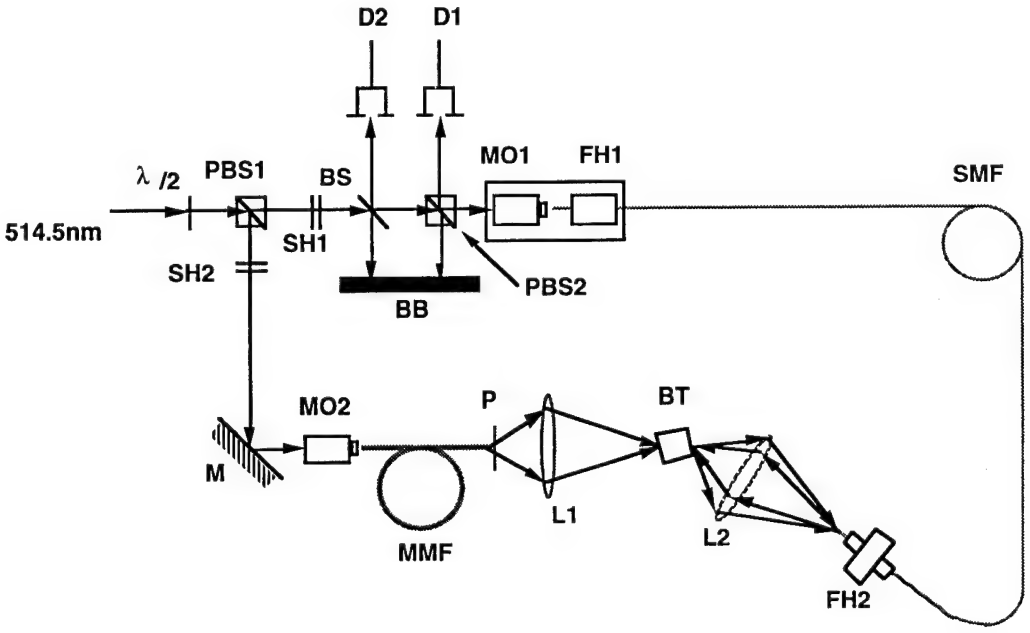

Fig. 17 An experimental configuration for the demonstration of fault-tolerant and efficient coupling of light from a multimode fiber into a singlemode fiber. λ/2: half-wave plate, PBS: polarizing beam splitter, SH: shutter, BS: beam splitter, D: detector, MO: microscope objective, FH: fiber holder, SMF: singlemode fiber, MMF: multimode fiber, M: mirror, BT: barium titanate crystal, L: lens, BB: beam blockage, P: polarizer.

For a given photorefractive crystal and a specific experimental geometry, the multimode to singlemode coupling efficiency depends on the beacon-to-signal power ratio. In our experiment, the optical power of the two beams injected into the crystal was varied in the range of 1 mW to 20 mW. A typical set of experimental data as depicted in Fig. 18 reveals the following points. 1) The polarization of the transmitted light is essentially horizontal (i.e., the polarization is preserved in the mode conversion and the transmission through the SMF). 2) The coupling efficiency peaks

when the beacon-to-signal power ratio is around 2, and decreases as the ratio increases. The maximum coupling efficiency achieved is about 15%. Another interesting point that we observed (which is not shown in Fig. 18) is that when the ratio is reduced to less than one, the coupling becomes unstable.

When the beacon beam was switched off (by shutter SH1 in Fig. 17), the signal transmitted through the SMF (as monitored by the detector D1) decayed slowly (~ a few seconds) as the photorefractive gratings responsible for the coupling were erased by the signal beam. The signal recovered at a much faster rate (in less than 1 second) when the beacon beam was switched on again, provided that the gratings were not severely erased (Fig. 19a). To further illustrate this point, an example in which the beacon beam was turned off for about 80 seconds was shown in Fig. 19b. In this example, the gratings were erased to such an extent that the coupling efficiency was reduced to less than 0.01% of the maximum value; the corresponding recovery time was much longer. The contrast ratio (i.e., the maximum transmitted power at the steady state/minimum transmitted power after the beacon beam is turned off and the gratings responsible for MPPC are completely erased), which is limited by the background stray light, is greater than 10^5.

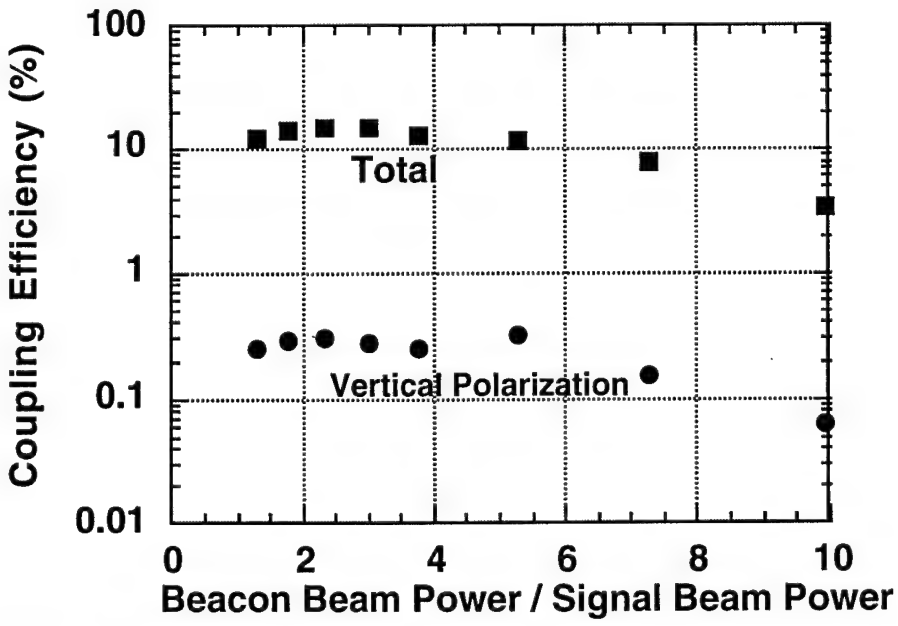

Fig. 18 Multimode to singlemode light coupling efficiency as a function of the power ratio of the beacon and the signal beams.

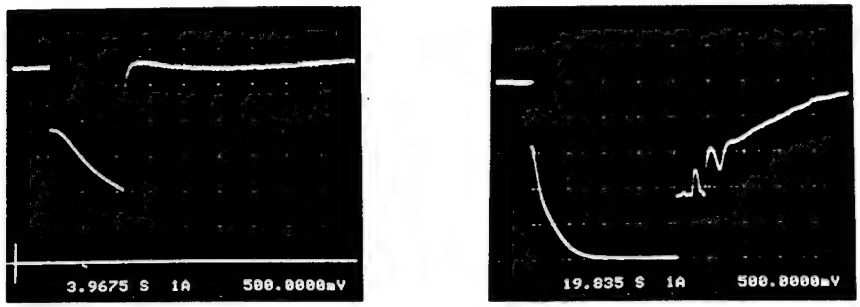

(a) (b)

(a) Residual Grating Strength ~ 54%
(b) Residual Grating Strength < 0.01%

Fig. 19 Oscillograms showing the decay and the recovery of the signal transmitted through the singlemode fiber when the beacon beam was switched off and on again at an instant when the transmitted power was (a) 54%, (b) 0.01% of the peak value.

In MPPC, both the signal and the beacon beams can be modulated simultaneously, each with its own modulation frequency, to form a two-way communication link. We have experimentally demonstrated that the modulation of the input beams does not prohibit the system to initiate and sustain a stable oscillation. As an example, a modulated signal transmitted into the SMF from the MMF was shown in Fig. 20 (a) for the case of a steady-state oscillation, and in Fig. 20 (b) for the case when the beacon beam was switched off and the photorefractive gratings were completely erased.

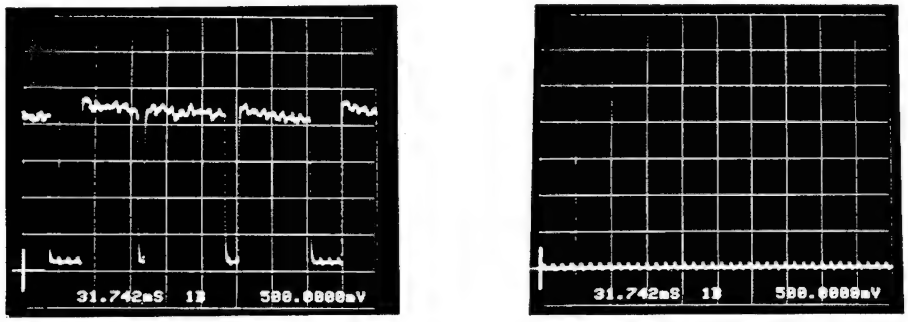

Signal with beacon beam "ON" **Signal with beacon beam "OFF"**

Fig. 20 Oscillograms showing the modulated signal transmitted into the SMF from the MMF; (a) at steady-state oscillation, (b) when the beacon beam was switched off and the photorefractive gratings were completely erased.

To demonstrate the degree of fault-tolerance of this novel coupling technique, the facet of the SMF was displaced horizontally by adjusting one of the micrometers of the five-axis fiber holder (FH2 in Fig. 17). The transmitted signal (monitored the detector D1) dropped abruptly and recovered slowly in about 40 seconds [see Fig. 21 (a)] as the original gratings were erased and new gratings were formed. The minima of the signal level in Fig. 21 (a) was limited by the back reflection of the beacon beam from the microscope objective (MO1) and the SMF. We observed a complete recovery of signal via self-healing even when the fiber facet was displaced by about 100 μm, which is more than 30 times the fiber core diameter. Likewise, we have also varied the vertical position and the angular orientation of the fiber facet and show that signal recovery applies to all six degrees of freedom. Experimental results for the vertical displacement of the fiber facet were shown in Fig. 21 (b). Note that the recovery time for the vertical displacement is significantly longer (approximately 4 to 6 times) than that for the horizontal displacement. This is again due to the fact that the beam fanning which is preferentially along the horizontal plane is much more efficient in generating new set of gratings within the same horizontal layer.

Experimental Result:
Fault-Tolerance (Self-Healing)
with respect to position of the fiber facet

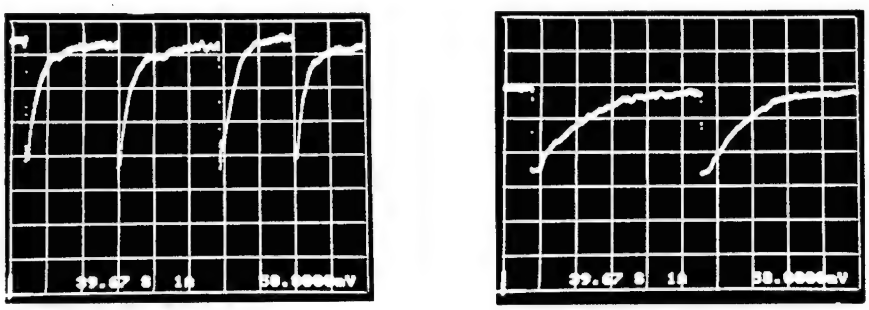

(a) (b)

SMF displaced (a) horizontally, (b) vertically

• Linear Fault-Tolerance > 30d

Fig. 21 Oscillograms showing the abrupt drop and the gradual recovery of the signal transmitted through the singlemode fiber when the fiber facet was displaced (a) horizontally, (b) vertically. The minima of the signal level represent the background due to back reflection of the beacon beam from the microscope objective and the fiber.

The 1/N limit for the coupling of light from a MMF into a SMF using the conventional technique (such as a single- or multiple- lens system) can be estimated by $(d/D)^2$, where d and D are the core

diameters of the SMF and the MMF, respectively. For d = 2.9 μm and D = 100 μm, $(d/D)^2$ ~ 0.084%. To compare with this crude estimation, a microscope objective (10x, NA = 0.30) was used to couple the output of the MMF directly into the SMF (mounted on the same five-axis fiber holder/aligner, FH2). The coupling efficiency was so sensitive to the position of the facet of the SMF that it was extremely difficult to maximize the output and hold the fiber facet at the optimum position. Typically, the coupling efficiency achieved was in the range of 0.01% to 0.08%. In contrast, the photorefractive technique described above consistently exhibits a coupling efficiency of about 15%, which is more than two orders of magnitude higher than the 1/N limit! The comparison described above is depicted in Fig. 22 where the coupling efficiency vs the number of modes (N) supported by the MMF is plotted for the conventional approach and the photorefractive approach based on MPPC. For $N > 10^4$, the coupling efficiency using MPPC is 3 to 4 orders of magnitude higher than that achievable by the conventional approach.

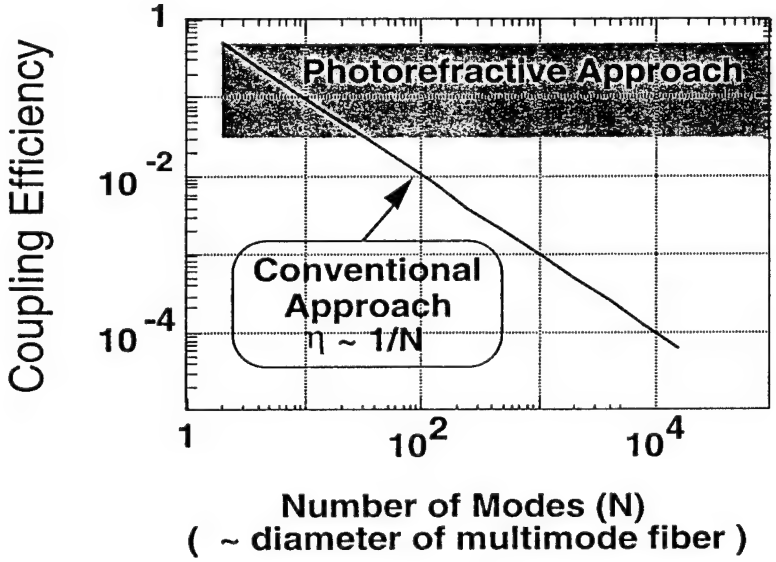

Fig. 22 A plot of coupling efficiency as a function of the number of modes for the comparison of the performance of multimode-to-singlemode fiber optic coupling using the conventional techniques vs the photorefractive approach based on MPPC.

4.0 Suggestion For Further Research and Development

In this program, we have clearly demonstrated the potential applications of two novel techniques for efficient and fault-tolerant laser-to-fiber and multimode-to-singlemode fiber-optic couplings. Both demonstrations were carried out using an argon ion laser at 514.5 nm together with a 45°-cut barium titanate crystal where the photorefractive coupling is known to be very strong. As a feasibility demonstration of laser-to-fiber coupling, we have used a large core diameter (400 μm) multimode fiber in stead of a single mode fiber. From the practical point of view, it is imperative to be able to extend the technique (using a semilinear phase conjugate resonator, or SPCR) to the coupling of a semiconductor laser diode output into a singlemode fiber. Whereas high gain photorefractive material such as barium titanate can cover the range of visible through near infrared (~ 0.4 μm to 1.1 μm), the response time is longer as the wavelength increases.[67] For wavelengths of interest in telecommunication (such as 1.3 μm and 1.5 μm), photorefractive semiconductors[68] such as indium phosphite (InP)[69, 70] or cadmium telluride (CdTe)[71] are by far the best candidates. However, the gain provided by these crystals is usually much smaller without an externally applied electric field.[69] Furthermore, for the case of coupling of light into a singlemode fiber using SPCR, treatment such as rear-facet coating or prerecording of a Bragg grating in the fiber core[63–66] (see Fig. 13) will become essential to match the oscillation mode to the fiber mode. An initial alignment with reasonable accuracy might also be required to provide sufficient feedback to trigger the oscillation. Once the grating is established, however, tolerance to angular misalignment (~ a few degrees) and/or linear misalignment (~ several fiber diameters) can be expected provided the rate of changes is slower than the photorefractive response time (which is typically on the order of tens of microseconds to milliseconds for photorefractive semiconductors). From the system point of view, the trade-off among several performance parameters includes the degree of fault-tolerance, maximum coupling efficiency, and the recovery time. Despite the concern expressed by some researchers on the applicability of this technique to couple light from semiconductor lasers to singlemode fibers due to the extremely small core diameter (on the order of a few microns to about 10 μm), the surrounding cladding (which has a typical diameter of a few hundred microns) may serve as an attractor to guide the initiation of the oscillation. Once the oscillation starts, the Bragg grating inside the core can provide sufficient optical feedback to defeat the cladding mode in the steady state. For the case of multimode-to-singlemode fiber optic coupling, experimental demonstrations at 1.3 μm using indium phosphite (with externally applied electric field) are quite feasible in the near term (~ 12 to 18 months). On a longer term (~ 24 to 36 months), investigation on the extension of this technique to the case

involving more than two channels for reconfigurable interconnection or wavelength division multiplexing (WDM) should be of interest to the fiber-optic communication industry. Last but certainly not least, research on photorefractive semiconductors (such as indium phosphite and cadmium telluride) to improve their coupling strength at the wavelength range of 13 μm to 1.5 μm will be very helpful to the advancement of these techniques.

5.0 References

1. P. Yeh, *Introduction to Photorefractive Nonlinear Optics* (John Wiley & Sons, Inc., New York, 1993).

2. D. Pepper, J. Feinberg, N. Kukhtarev, "The photorefractive effect", *Scientific Am.* 62–72 (1990).

3. P. Gunter, J.-P. Huignard, "Photorefractive Effects and Materials", in *Photorefractive Materials and Their Applications I: Fundamental Phenomena*, P. Gunter, J.-P. Huignard, Eds. (Springer-Verlag, Berlin, Heidelberg, 1988), pp. 7–73.

4. N.V. Kukhtarev, V.B. Markov, S.G. Odulov, M.S. Soskin, V.L. Vinetskii, "Holographic storage in electro-optic crystals I. steady state", *Ferroelectrics* **22**, 949–964 (1979).

5. N.V. Kukhtarev, V.B. Markov, S.G. Odulov, M.S. Soskin, V.L. Vinetskii, "Holographic storage in electro-optic crystals. II. beam coupling–light amplification," *Ferroelectrics* **22**, 961 (1979).

6. P. Gunter, J.-P. Huignard, in *Topics in Applied Physics* (Springer-Verlag, Berlin, Heidelberg, 1988), pp. 295.

7. P. Gunter, J.-P. Huignard, in *Topics in Applied Physics* (Springer-Verlag, Berlin, Heidelberg, 1989), pp. 367.

8. G.C. Valley, M.B. Klein, R.A. Mullen, R. Rytz, B. Wechsler, "Photorefractive materials", *Ann. Rev. Mater. Sci.* **18**, 165–188 (1988).

9. N. Sonderer, P. Gunter, "Near infrared nonlinear optical phase conjugation in photorefractive crystals and semiconductor materials–Part II: Materials and applications", *Int. J. Nonlinear Opt. Phys.* **3**, 373–438 (1994).

10. P. Yeh, "Two-wave mixing in nonlinear media," IEEE J. Quantum Electron. **25**, 484-519 (1989).

11. Y. Fainman, E. Klancnik, S.H. Lee, "Optimal coherent image amplification by two-wave coupling in photorefractive $BaTiO_3$", *Opt. Eng.* **25**, 228–234 (1986).

12. J. Hong, A. Chiou, P. Yeh, "Image amplification by two-wave mixing in photorefractive crystals", *Appl. Opt.* **29**, 3026–3029 (1990).

13. H. Rajbenbach, A. Delboulbe, J.-P. Huignard, "Low-noise amplification of ultraweak optical wave fronts in photorefractive $Bi_{12}SiO_{20}$", *Opt. Lett.* **16**, 1483 (1991).

14. T.Y. Chang, J.H. Hong, P. Yeh, "Spatial amplification: an image-processing techniques using the selective amplification of spatial frequencies", *Opt. Lett.* **15**, 743–745 (1990).

15. T.Y. Chang, J. Hong, in *CLEO'93* (Optical Society of America, Baltimore, MD, 1993), pp. 630–632.

16. A. Chiou, P. Yeh, "Parallel image substraction using a phase-conjugate Michelson interferometer", *Opt. Lett.* **11**, 306–308 (1986).

17. M. Cronin-Golomb, A. M. Biernacki, C. Lin, H. Kong, "Photorefractive time differentiation of coherent optical image", *Opt. Lett.* **12**, 1029–1031 (1987).

18. F. Ito, K. Kitayama, "Distrotation free reconstruction through phase conjugation of holographic image in photorefractive crystal waveguide", *IEICE Trans. Electron.* **E75-C**, 741–743 (1992).

19. Y.H. Ja, "Real-time image deblurring using four-wave mixing"," *Opt. and Quantum Electron.* **15**, 457–459 (1983).

20. S.-Z. Kwong, G.A. Rakulic, V. Leyva, A. Yariv, "Real time image processing using a self-pumped phase conjugate mirror", *SPIE Proc.* **613**, 36–42 (1986).

21. C. Uhrich, L. Hesselink, "Submicrometer defect enhancement in periodic structures by using photorefractive holography", *Opt. Lett.* **17**, 1087–1089 (1992).

22. J. White, A. Yariv, "Real-time image processing via four-wave mixing in a photorefractive medium", *Appl. Phys. Lett.* **37**, 5–7 (1980).

23. J.E. Ford, S.H. Lee, Y. Fainman, "Applications of photorefractive crystals to optical interconnection", *Proc. SPIE* **1215**, 155–165 (1990).

24. S. Weiss, M. Segev, S. Sternklar, B. Fischer, "Photorefractive dynamic optical interconnects", *Appl. Opt.* **27**, 3422–3428 (1988).

25. S. Wu, Q. Song, A. Mayers, D.A. Gregory, F.T. S. Yu, "Reconfigurable Interconnections Using Photorefractive Holograms", *Appl. Opt.* **29**, 1118–1125 (1990).

26. A. Chiou, P. Yeh, S. Campbell, J. Hong, "Reconfigurable optical interconnection using photorefractive holograms", in *Proc. SPIE* (1989), pp. 24–32.

27. A. Chiou, P. Yeh, "Energy efficiency of optical interconnections using photorefractive dynamic holograms", *Appl. Opt.* **29**, 1111–1117 (1990).

28. A. Chiou, P. Yeh, in *Conference of Lasers and Electro-Optics (CLEO) '92* (Optical Society of America, Washington, D.C.; Anaheim, California, 1992), pp. 60.

29. A. Marrahchi, W.M. Hubbard, S.F. Harbiby, J.S. Patel, "Dynamic holographic interconnect with analog weights in photorefractive crystals", *Opt. Eng.* **29**, 215–224 (1990).

30. A.A. Kamshilim, *et al.*, "Two-wave mixing in photorefractive $Bi_{12}SiO_{20}$ fibers", *Opt. Lett.* **18**, 690–692 (1993).

31. L. Hesselink, "New applications for photorefractive fibers", *Opt. and Photonics News* **4**, 9–15 (1993).

32. K.E. Youden, *et al.*, "Photorefractive planar waveguides in $BaTiO_3$ fabricated by ion-beam implantation", *Opt. Lett.* **17**, 1509–1511 (1992).

33. F. Ito, K. Kitayama, "Photorefractive crystal waveguide with periodically reversed c axis for enhanced two-wave mixing", *Appl. Phys. Lett.* **59**, 1932–1934 (1991).

34. B. Fischer, M. Segev, "Photorefractive waveguides and nonlinear mode coupling effects", *Appl. Phys. Lett.* **54**, 684–686 (1989).

35. A. Chiou, P. Yeh, C. Gu, R. Neurgaonkar, in *IEEE LEOS'93 Conference Proceedings* (IEEE, Piscataway, NJ; San Jose, CA, 1993), pp. 319–320.

36. A. Chiou, P. Yeh, C. Gu, in *OSA Annual Meeting Technical Digest Series* (Optical Society of America, Washington, D.C.; Toronto, Ontario, Canada, 1993), pp. 7.

37. M. Segev, Y. Ophir, B. Fischer, "Photorefractive self-defocusing", *Appl. Phys. Lett.* **56**, 1086–1088 (1990).

38. B. Crosignani, *et al.*, "Self-trapping of optical beams in photorefractive media", *J. Opt. Soc. Am. B* **10**, 446–453 (1993).

39. J.G. C. Duree, *et al.*, "Observation of self-trapping of an optical beam due to the photorefractive effect", *Phys. Rev. Lett.* **71**, 533–536 (1993).

40. J. Feinberg, "Asymmetric self-defocusing of an optical beam from the photorefractive effect", *J. Opt. Soc. Am.* **72**, 46–51 (1982).

41. M. Cronin-Golomb, A. Yariv, "Optical limiters using photorefractive nonlinearities", *J. Appl. Phys.* **57**, 4906–4910 (1985).

42. M.B. Klein, G.J. Dunning, "Performance optimization of photorefractive excisors", *Proc. SPIE* **1692**, 73–77 (1992).

43. D.Z. Anderson, J. Feinberg, "Optical novelty filter", *IEEE J. Quantum. Electron.* **25**, 635–647 (1989).

44. J. Joseph, P.K. C. Pillai, K. Singh, "High-gain, low-noise signal beam amplification in photorefractive $BaTiO_3$", *Appl. Opt.* **30**, 3315–3318 (1991).

45. W.S. Rabinovich, B.J. Feldman, G.C. Gilbreath, "Suppression of photorefractive beam fanning using achromatic grating", *Opt. Lett.* **16**, 1147–1149 (1991).

46. H. Rajbenbach, A. Delboulbe, J.-P. Huignard, "Noise suppression in photorefractive image amplifiers", *Opt. Lett.* **14**, 1275–1277 (1989).

47. M. Cronin-Golomb, B. Fischer, J.O. White, A. Yariv, "Passive (self-pumped) phase conjugate mirror: Theoretical and experimental investigation", *Appl. Phys. Lett.* **41**, 689–691 (1982).

48. M. Cronin-Golomb, B. Fischer, J. Nilsen, J.O. White, A. Yariv, "Laser with dynamic holographic intracavity distortion correction capability", *Appl. Phys. Lett.* **41**, 219–220 (1982).

49. M. Cronin-Golomb, B. Fischer, J.O. White, A. Yariv, "Passive phase conjugate mirror based on self-induced oscillation in an optical ring cavity", *Appl. Phys. Lett.* **42**, 919–921 (1983).

50. P. Gunter, "Holography, coherent light amplification and optical phase conjugation with photorefractive materials", *Phy. Rep.* **93**, 199–299 (1982).

51. A. Yariv, "Phase conjugate optics and real-time holography", *IEEE J. Quantum Electron.* **QE-14**, 650–660 (1978).

52. J. Feinberg, "Optical phase conjugation in photorefractive materials", in *Optical Phase Conjugation*, R.A. Fisher, Eds. (Academic Press, New York, 1983), pp. 417–443.

53. J.A. Schuenke, "A novel technique for laser diode to single mode fiber coupling", *Fiber and Integrated Opt.* **6**, 191–201 (1987).

54. E. Jaatinen, B. Luther-Davies, "Converting 10kW multi-mode fields into a single spatial mode with a semilinear phase conjugate mirror", *Int. J. Nonlinear Opt. Phys.* **3**, 117–125 (1994).

55. M.D. Ewbank, "Mechanism for photorefractive phase conjugation using incoherent beams", *Opt. Lett.* **13**, 47–49 (1988).

56. B. Fischer, S. Sternklar, S. Weiss, "Photorefractive oscillator", *IEEE J. Quantum Electron.* **QE-25**, 550–568 (1989).

57. E.J. Sharp, *et al.*, "Double phase conjugation in tungsten bronze crystals", *Appl. Opt.* **29**, 743–749 (1990).

58. S. Sternklar, B. Fischer, "Double-color-pumped photorefractive oscillator and image color conversion", *Opt. Lett.* **12**, 711–713 (1987).

59. Q.B. He, "Photorefractive mutually pumped phase conjugators", in *Photorefractive Materials, Effects, and Applications*, P. Yeh, C. Gu, Eds. (SPIE, Bellingham, 1993), pp. 59–75.

60. M.P. Schamschula, H.J. Caulfield, C.M. Verber, "Adaptive optical interconnection", *Opt. Lett.* **16**, 1421–1423 (1991).

61. M. Snowbell, N. Strasman, B. Fischer, M. Cronin-Golomb, "Efficient self-aligning multibeam coupling into a single-mode fiber", *J. Lightwave Tech.* **13**, 55–61 (1995).

62. M. Cronin-Golomb, "Dynamically programmable self-aligning optical interconnect with fan-out and fan-in using self-pumped phase conjugations", *Appl. Phys. Lett.* **54**, 2189–2191 (1989).

63. L. Dong, J.L. Archambault, L. Reekie, P.S.J. Russell, D.N. Payne, "Bragg grating in Ce3+-doped fibers written by a single excimer pulse", *Opt. Lett.* **18**, 861–863 (1993).

64. K.O. Hill, "Photosensitivity in optical fibers", *Ann. Rev. Mater. Sci.* **23**, 125–157 (1993).

65. K.O. Hill, B. Malo, K.A. Vineberg, D.C. Johnson, I. Skinner, "Efficient mode conversion in telecommunication fiber using externally written gratings", *Electron. Lett.* **26**, 1270–1272 (1990).

66. G. Meltz, W.W. Morey, W.H. Glenn, "Formation of Bragg gratings in optical fibers by a transverse holographic method", *Opt. Lett.* **14**, 823–825 (1989).

67. M. Cronin-Golomb, "Infrared photorefractive passive phase conjugator with $BaTiO_3$: Demonstration with GaAlAs and 1.09-μm Ar^+ lasers", *Appl. Phys. Lett.* **47**, 567–569 (1985).

68. N. Sonderer, P. Gunter, "Near infrared nonlinear optical phase conjugation in photorefractive crystals and semiconductor materials–Part I: Fundamentals", *Int. J. Nonlinear Opt. Phys.* ***3***, 225–275 (1994).

69. R.B. Bylsma, A.M. Glass, D.H. Olson, "Optical signal amplification at 1.3 μm by two-wave mixing in InP:Fe", *Electron. Lett.* **24**, 360–362 (1988).

70. J. Strait, J.D. Reed, A. Saunders, G.C. Valley, M.B. Klein, "Net gain in photorefractive InP:Fe at $\lambda = 1.32$ μm without an applied field", *Appl. Phys. Lett.* **57**, 951–953 (1990).

71. A. Partovi, *et al.*, "Photorefractivity at 1.5 μm in CdTe:V", *Appl. Phys. Lett.* **57**, 846–848 (1990).

6.0 Appendix

6.1 A. Chiou, P. Yeh, and C. Gu, "Spatial mode conversion in photorefractive fibers", in OSA Annual Meeting Technical Digest, 1993 (Optical Society of America, Washington, D.C., 1993), Vol. 16, pp. 7.

6.2 A. Chiou, P. Yeh, C. Gu, and R. Neurgaonkar, "Beam coupling and spatial mode conversion in photorefractive planar waveguide", IEEE LEOS'93 Conference Proceedings, San Jose, November 1993, pp. 319.

6.3 A. Chiou, P. Yeh, C.-X. Yang, and C. Gu, "Photorefractive coupler for fault-tolerant coupling", to appear in *Photonics Tech. Lett.* July 1995.

6.4 A. Chiou, P. Yeh and C. Gu, "A photorefractive spatial mode converter for multimode to singlemode fiber-optic coupling", to appear in *Opt. Lett.* May 1995.

Appendix 6.1

A. Chiou, P. Yeh, and C. Gu, "Spatial mode conversion in photorefractive fibers", in OSA Annual Meeting Technical Digest, 1993 (Optical Society of America, Washington, D.C., 1993), Vol. 16, pp. 7.

MD8 9:45 am

Spatial mode conversion in photorefractive fibers, Arthur Chiou, Pochi Yeh,* Claire Gu** *Rockwell International Science Center, 1049 Camino Dos Rios, Thousand Oaks, CA 91360. aechiou@scimail.remnet.rockwell.com.* Photorefractive fibers have been successfully grown[1,2] and studied for optical storage[3] and optical interconnection and switching.[4] The a-axis fibers have attracted much more attention (relative to the c-axis fibers) for potential applications in optical storage and interconnection. The c-axis fibers, however, have the unique capability of converting the optical energy (propagating inside the fibers) from the higher order spatial modes into lower order modes.[5,6] Such a mode conversion is potentially useful for fault-tolerant laser-to-fiber coupling.[6] A simple theoretical model, which assumes equal coupling coefficient Γ between any two modes, indicates that all the energy will be transferred to the fundamental mode, provided that ΓL (where L is the length of the fiber) is sufficiently large. In this paper, we present our theoretical results for spatial mode conversion, together with the corresponding experimental results using c-axis fiber samples of Fe-doped lithium niobate and Ce-doped strontium barium niobate. In addition, we discuss the novel concept of the applications of spatial mode conversion in photorefractive fibers for efficient and fault-tolerant laser-to-fiber coupling. This work is supported by DARPA/AFOSR under contract number F49620-92-C-0067.

1. J. P. Wilde, D. H. Jundt, L. Galambos, and L. Hesselink, J. Crystal Growth **114**, 500 (1991).
2. Y. Sugiyama, I. Yokohama, K. Kubodera, and S. Yagi, IEEE Photon. Technol. Lett. **3**, 744 (1991).
3. L. Hesselink, Int. J. of Optoelectron. **5**, 103 (1990).
4. S. Wu, A. Mayers, S. Rajan, and F. T. S. Yu, Appl. Opt. **29**, 1059 (1990).
5. M. Segev, Y. Ophir, and B. Fischer, Appl. Phys. Lett. **56**, 1086 (1990).
6. P. Yeh, Proc. SPIE **1582**, 3 (1991).

*University of California, Santa Barbara, CA 93106.

**The Pennsylvania State University, University Park, PA 16802.

MD9 10:00 am

Photorefractive, photovoltaic and thermal contributions to beam fanning in $LiNbO_3$, Partha P. Banerjee, Jaw-Jueh Liu, *Department of Electrical and Computer Engineering, University of Alabama in Huntsville, Huntsville, AL 35899, banerjee@ebs330.eb.uah.edu.* We study steady state deterministic beam fanning (DBF) in the far-field in $LiNbO_3$ both experimentally and theoretically when an ordinary polarized Gaussian beam is externally focussed into the material. Our measurements of DBF are performed using a $LiNbO_3$:Fe (0.01 wt. %) crystal of dimensions 10 mm × 10 mm × 10mm. To analyze the effect, we derive a closed form expression for the induced refractive index change from the nonlinearly coupled Kukhtarev equations[1] by including both the photorefractive (PR) and photovoltaic (PV) effects, as well as heuristically adding the thermal effect[2] in the calculations. By using a split-step beam propagation method,[3] we account for the effect of propagational diffraction in the spatial frequency domain, while the effects of induced nonlinearity are accounted for in the spatial domain. The temperature profile is recalculated at every step during propagation by using a spatial Fourier transform technique. Our results show that, generally speaking, as the focussed spot size w_0 increases or the beam power decreases, DBF decreases. Over ranges of our experiments and calculations, PV and thermal effects are more dominant than the PR effect. There is a reasonably good agreement between theory and experiment over the selected range of w_0 and power.

1. N. V. Kukhtarev, V. B. Markov, S. G. Odulov, M. S. Soskin, and V. L. Vinetski, Ferroelectrics **22**, 949 (1979).
2. I. P. Gordon, R. C. C. Leite, R. S. Moore, S. P. S. Porto, and J. R. Whinnery, J. Appl. Phys. **36**, 3 (1965).
3. A. Korpel, K.E. Lonngren, P.P. Banerjee, H.K. Sim, and M.R. Chatterjee, J. Opt. Soc. Amer. B **3**, 885 (1986).

ME 8:00 am 203A/B

Symposium on Laser Material Processing Delivery Systems

R. Edward English, *Lawrence Livermore National Laboratory, Presider*

ME1 (Invited) 8:00 am

Trends in fiber-optic beam delivery for materials processing, Thomas R. Kugler, *Lumonics Corporation, 1977o Haggerty Road, Livonia, MI 48152-1016.* The initial application of fiber optic delivery to materials processing can be traced back to the early 1980s. These early uses were somewhat conservative and served as ground breaking attempts by the designers to test the life and construction of fiber components. Advantages abounded and the longevity of these devices were found to be extremely good. Power levels were increased and modular systems designed as well as special layouts. Higher powers have brought out concerns but safety innovations have been developed to keep pace. At the present time, laser design itself is determined by fiber capability. The use of fiber systems has made the Nd:YAG laser more widely used and opened-up applications that were impossible a few years ago. These topics will be discussed and related to actual hardware and applications in use today.

ME2 (Invited) 8:30 am

Fiber delivered cw Nd:YAG laser systems with powers as high as 3 kW and their applications, David M. Filgas, *Hobart Laser Products, 332 Earhart Way, Livermore, CA 94550.* Recent advances in high power cw Nd:YAG lasers and fiberoptic beam delivery have resulted in commercial systems with powers up to 3 KW. This opens the door for a variety of new applications and provides great improvements in processing rates for many existing applications This paper will discuss the features, performance, and applications of systems ranging from 600W to 3 KW with delivery via 600 micron fiber. Multiplexing the laser energy between up to 4 fibers permits utilization of one laser by multiple workstations. In contrast, the fiber delivered outputs of several lasers can be combined at a single workpiece for processing at up to 9 KW. Long distance fiber delivery, up to 150m, permits processing in remote locations. Fiber to fiber coupling allows the use of short disposable fibers in hazardous environments. Due to these features, and the inherent flexibility of fiber delivery, the number of applications is growing rapidly. Excellent performance has been achieved in cutting, welding, cladding, surface hardening, and paint stripping. Applications of particular interest are three dimensional robotic cutting, lap welding of galvanized steel, and butt welding of custom blanks.

Appendix 6.2

A. Chiou, P. Yeh, C. Gu, and R. Neurgaonkar, "Beam coupling and spatial mode conversion in photorefractive planar waveguide", IEEE LEOS'93 Conference Proceedings, San Jose, November 1993, pp. 319.

9:30am - 9:45am
NLO4.3

Room B2

Beam Coupling and Spatial Mode Conversion in Photorefractive Planar Waveguide

Arthur Chiou, Pochi Yeh*, Claire Gu**, and Ratnakar Neurgaonkar

Rockwell International Science Center, Thousand Oaks, CA 91360
* University of California, Santa Barbara, CA
** Penn State University, University Park, PA

Beam coupling in photorefractive bulk crystals has been studied intensively and demonstrated for many application concepts, including coherent image amplification, image processing and parallel logic operations.[1] In contrast, photorefractive beam coupling and spatial mode conversion in guided wave structures have attracted much less attention.[2-6] The latter has potential application in facilitating the coupling of a free propagating laser beam to low-order guided modes in an appropriate waveguide structure.[7] In this paper, we discuss this novel concept and present experimental demonstrations of beam coupling and spatial mode conversion in a thin plate of strontium barium niobate (SBN:75) crystal.

In a multimode waveguide or fiber, a higher order mode can be represented by a wave-vector $\mathbf{K}_2$ propagating at an angle θ_2 (relative to the fiber axis) which is larger than the corresponding angle θ_1 associated with a lower order mode (Fig.1a). If the fiber is made of photorefractive material with c-axis parallel to the fiber axis, energy can be transferred from the higher order to the lower order modes via photorefractive beam coupling as the optical wave propagates towards the "+c" direction (Fig.1b). In principle, if the product of the coupling constant and the interaction length (ΓL) is sufficiently large (and assuming negligible loss), all the energy will eventually be transferred to the lowest order mode. In addition, the dynamic nature of the photorefractive grating can adaptively correct for certain changes in the input beam geometries such as the direction of beam injection and the beam profile. This process can therefore facilitate the coupling of a laser beam to a fiber or waveguide by not only improving the coupling efficiency but also reducing the sensitivity to misalignment.

In the following, we describe the experimental configurations and discuss the experimental results of beam coupling and mode conversion in a one-dimensional geometry using a photorefractive planar waveguide. The sample is a regular (xyz) cut SBN:75 plate (~9mmx10mmx1mm) with c-axis lying along the large a-face. Both a- and c- faces are optically polished.

For the study of multiple-beam coupling in discrete modes, four parallel beams originating from an argon laser (514.5nm) were focused and coupled into the plate from the c-face at different angle of incidence via a focusing lens L (f = 63mm) as illustrated in Fig.2a. The output of the signal beam (i.e., the one parallel to the c-axis) was monitored by a detector. When the beams are injected towards the "+c" direction, energy transfer from the other beams into the signal beam, and vice versa, was observed.

For the study of spatial mode conversion in a continuum of K-vectors, the four discrete beams were replaced by an expanded sheet of beams via appropriate cylindrical optics (Fig.2b). The fact that the mode conversion (from the higher order to the lower order, or vice versa) is due to photorefractive dynamic grating is verified by introducing a strong erasure beam (with polarization orthogonal to that of the signal beam) from the a-face.

As the erasure beam was turned on, the coupling decayed with the characteristic photorefractive time constant. The output signals with and without the presence of the erasure beam are shown in Fig.3. Quantitative characterization of the phenomena described above will be presented.

This work is supported by ARPA/AFOSR under contract No. F49620-92-0067.

References:

1. See, for example, P. Yeh, *Introduction to Photorefractive Nonlinear Optics* (Wiley, New York, 1993).
2. B. Fischer and M. Segev, "Photorefractive waveguides and nonlinear mode coupling effects," Appl. Phys. Lett. **54**, 684 (1989).
3. F. Ito and K. Kitayama, "Photorefractive crystal waveguide with periodically reversed c axis for enhanced two-wave mixing," Appl. Phys. Lett. **59**, 1932 (1991).
4. K. E. Youden, et al., "Photorefractive planar waveguides in $BaTiO_3$ fabricated by ion-beam implantation," Opt. Lett. **17**, 1509 (1992).
5. A. A. Kamshilin, et al., "Two-wave mixing in photorefractive $Bi_{12}SiO_{20}$ fibers," Opt. Lett. **18**, 690 (1993).
6. M. Zha, et al., "Two-wave mixing in photorefractive ion-implanted $KNbO_3$ planar waveguides at visible and near-infrared wavelengths," Opt. Lett. **18**, 577 (1993).
7. P. Yeh, "Reconfigurable optical interconnection," Proc. SPIE **1582**, 3 (1991).

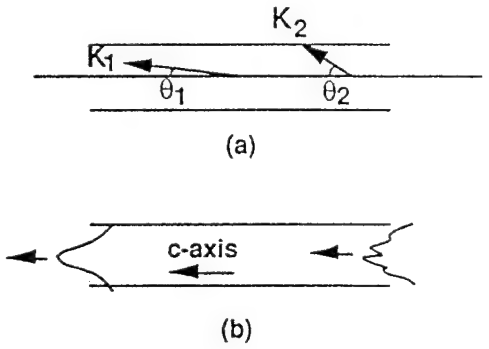

Fig.1 (a) Geometrical representation of wave-vectors associated with higher-order and lower-order modes in a multimode waveguide; (b) a conceptual illustration of spatial mode conversion in a photorefractive waveguide.

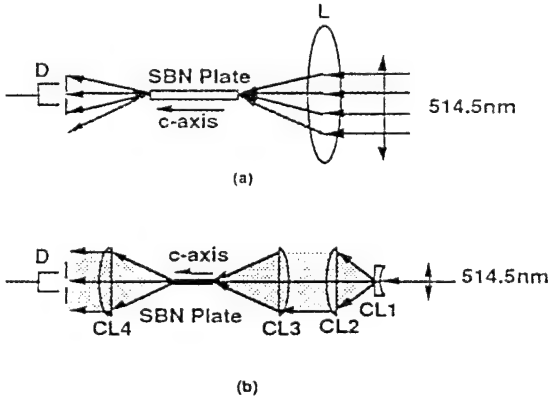

Fig.2 Experimental geometry for (a) beam coupling in discrete modes, (b) mode conversion in a continuum of K-vectors in a photorefractive planar waveguide.

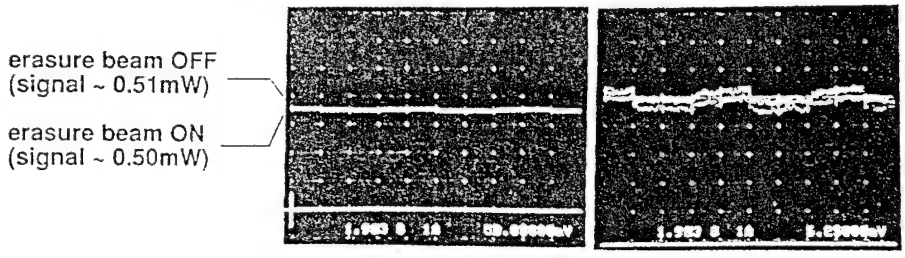

Fig. 3 Experimental results, corresponding to Fig. 2(b), showing the signal output with and without spatial mode conversion. The oscillograph on the right is a magnified (8x) version of the one on the left.

Appendix 6.3

A. Chiou, P. Yeh, C.-X. Yang, and C. Gu, "Photorefractive coupler for fault-tolerant coupling", to appear in *Photonics Tech. Lett.* July 1995.

Photorefractive coupler for fault-tolerant coupling

Arthur Chiou, Pochi Yeh*, Chang-Xi Yang*, Claire Gu**,
Rockwell International Science Center
1049, Camino Dos Rios, Thousand Oaks, CA 91360
Tel: (805)373-4464
Fax:(805)373-4775
Internet: aechiou@scimail.remnet.rockwell.com

* Electrical & Computer Engineering Dept., University of California at Santa Barbara, Santa Barbara, CA 93106
** Electrical Engineering Dept., Penn State University, University Park, PA 16802

Abstract

We report the first experimental demonstration of a fault-tolerant laser-to-fiber coupler which is insensitive to both angular and lateral misalignments. Fault-tolerance is achieved by sending a laser beam into a photorefractive crystal which automatically senses and tracks the location of the fiber facet, and diffracts the input beam (via self-generated adaptive dynamic holograms) into the fiber. Using an argon laser (514.5nm), a barium titanate crystal and a multimode fiber (core diameter = 400μm, NA=0.16), we have achieved a coupling efficiency of 58% and a tolerance of more than 0.5mm of lateral misalignment. Techniques to improve the coupling efficiency and the degree of fault-tolerance, and to extend this method for the coupling of a laser diode output into a single mode fiber are discussed.

1. Introduction

Conventional techniques using optical elements such as spherical lenses, graded index lenses, confocal lens systems or tapered hemispherical fibers for the coupling of light from a laser diode to an optical fiber suffer from the drawback that the coupling efficiency is extremely sensitive to both angular and lateral misalignments.[1] For the case of a single mode fiber, for example, a relative displacement of about 1μm from the optimum coupling position can reduce the coupling efficiency by more than 3dB.[2] In this letter, we report the first experimental demonstration of adaptive fault-tolerant coupling from a laser to a multimode fiber with the aid of a photorefractive semilinear phase conjugate resonator (PSPCR)[3, 4] which uses the fiber as an output coupler. The photorefractive resonator pumped by an injected laser beam automatically senses and tracks the location of the fiber facet and directs the input beam into the fiber. In what follows, we describe the technical background, the principle of operation, the experimental procedure and results, and discuss several issues associated with the practical implementation of this technique.

2. Technical Background and Principle of Operation

When a laser beam with an appropriate wavelength and polarization enters a photorefractive crystal, the intensity distribution of the beam at the exit face of the crystal usually exhibits a characteristic fan shape. Such a phenomenon, known as beam fanning,[5] can be used to realize a PSPCR by placing a reflector along the fanning direction as shown in Fig.1.[4, 6, 7] Recently, such an arrangement has been used to demonstrate the conversion of a multimode field into a single spatial (free-propagating) mode.[8] The idea of replacing the reflector in a PSPCR with the facet of an optical fiber for laser-to-fiber coupling was first proposed and analyzed by Schuenke in 1987.[9] However, no experimental evidence has ever been reported to date.

In this letter, we report the first experimental demonstration of a fault-tolerant laser-to-fiber coupler that is based on a PSPCR with the entrance facet of the fiber as a partial reflector. We have shown that a small amount of light reflected back from the fiber can enhance selected sets of the fan gratings formed inside the photorefractive crystal and initiate the oscillation to form a PSPCR.[4] As the oscillation builds up from the feedback into the noise grating, the fanning pattern collapses into an oscillation mode of the resonator defined by the fiber facet, and a phase conjugate signal of the input beam

increases from zero to a steady-state value, while the light transmitted through the fiber also increases from an initial value to a much higher steady-state value. When the front end of the fiber is displaced or tilted (within a certain range) to a new location (or orientation), both the phase conjugate and the transmitted signals drop abruptly. However, after a certain characteristic time (on the order of a few seconds to a few minutes, depending on the experimental condition) new gratings are formed (as the old ones are erased) and both signals recover back to their steady-state values. In this novel approach, the coupling of light from the laser to the fiber is, therefore, adaptive and fault-tolerant. Note that the technique described in this paper is significantly different from those based on mutually-pumped phase conjugation which requires a beacon beam to be transmitted from the opposite end of the fiber.[10]

3. Experimental Configuration

The experimental configuration is illustrated schematically in Fig. 2. The output from an argon ion laser (514.5nm, and with horizontal polarization) was injected into a 45°-cut barium titanate crystal (5.6mmx5.5mmx5.9mm) with an angle of incidence of about 11°. The transmitted beam fanned preferentially along the direction of the c-axis as shown in the figure. The fanning beams were loosely focused by a focusing lens (FL, focal length =38mm, diameter = 50mm) to one facet of a glass fiber (core diameter = 400μm, cladding diameter = 500μm, numerical aperture = 0.16, length = 4m) mounted on a gimbal mount (not shown in the figure) so that its position/orientation can be adjusted in five degrees of freedom. The orientation of the entrance face of the fiber was adjusted manually so that the reflected light approximately retraced its incoming path back to the crystal. To provide sufficient optical feedback to assist the initiation of the oscillation, the entrance face of the fiber was polished and coated with thin alternating layers of TiO_2 and SiO_2 so that the Fresnel reflection at 514.5nm was about 36%. A beam splitter BS was placed in the front end of the crystal to sample the phase conjugate beam for monitoring by a detector D2. At the exit face of the fiber, the transmitted optical power was monitored by another detector D1.

4. Experimental Results and Discussion

In the initial state, when the input beam (~29mW) was first injected into the crystal, it began to fan towards the focusing lens, and the light coupling efficiency through the fiber was relatively low (about a few percent, depending on the exact location and orientation

of the entrance face of the fiber). During this period, no phase conjugate signal was detected. After a period ranging from a few seconds to a few minutes (depending on the experimental condition), as some selected sets of fanning gratings were gradually enhanced by the reflected light and its diffracted components, both the phase conjugate and the transmitted signals increased to some steady state values. A small change in either the position or the orientation of the entrance face of the fiber resulted in an abrupt drop of both signals followed by a slow recovery of both back to their steady state values. An example of the transmitted and the phase conjugate signals (upper trace for output from detector D1 and lower trace for that from D2) at the steady state and as the entrance face for the fiber was displaced transversely first by 250μm, and then followed by another 250μm, was shown in Fig. 3. Note that the total displacement was larger than the diameter of the fiber core which is 400μm. In addition to linear displacement, we investigated the effect of angular misalignment by changing the orientation of the fiber facet (or the crystal) by a few degrees. Our experimental results (similar to that shown in Fig. 3) confirm that the system is indeed insensitive to angular misalignment.

In the preliminary experiment, the coupling efficiency (defined as the output optical power transmitted through the fiber divided by the input optical power at the entrance face of the fiber) at the steady state was about 58% and the corresponding phase conjugate reflectivity (defined as the ratio of the optical power of the phase conjugate beam to the input optical power at the entrance face of the crystal) was about 1.3%. However, the net coupling efficiency (defined as the output optical power transmitted through the fiber divided by input optical power at the entrance face of the crystal) was only 20%. Loss of optical power (in dB) in each stage is indicated in the lower part of Fig. 2. Key factors that contribute to the energy loss include the Fresnel reflection at the front and back faces of the crystal (~ 0.8dB), absorption inside the crystal (~ 2.0dB), incomplete pump depletion (~ 0.4dB), energy loss at the focusing lens (~ 1.3dB), and energy loss in coupling into the fiber (~ 2.4dB). Of these factors, the Fresnel loss can be eliminated by antireflection coating the crystal faces, absorption inside the crystal can be reduced and pump depletion can be improved by proper selection (or doping and oxidation/reduction) of the crystal and/or the wavelength. Energy loss at the focusing lens can be reduced by using a lens with higher numerical aperture and/or a photorefractive crystal with smaller beam-fanning cone angle. Energy loss in coupling into the fiber can be reduced by optimizing the amount of light reflected back from the fiber. Although the optical feedback required for the oscillation can be provided by Fresnel reflection from either the entrance facet or the exit facet of the fiber or from an

appropriate Bragg grating recorded in the core of the fiber,[11] only reflection from the exit facet or from the Bragg grating recorded in the core of the fiber can automatically fulfill the mode matching condition. In both cases, the reflectivity needs to be optimized to achieve maximum coupling efficiency.

From the practical point of view, it is desirable to extend the technique to the coupling of a laser diode output into a single mode fiber. Whereas high gain photorefractive material such as barium titanate can cover the range of visible through near infrared (~ 0.4μm to 1.1μm), the response time is slower as the wavelength increases.[12] For wavelengths of interest in long distant telecommunication (such as 1.3μm and 1.5μm), photorefractive semiconductors such as indium phosphite (InP)[13, 14] or cadmium telluride (CdTe)[15] can be used. However, the gain provided by the latter is usually smaller without an externally applied electric field.[13] For the case of a singlemode fiber, treatment such as rear-facet coating or prerecording of a Bragg grating in the fiber core[11] is required to match the oscillation mode to the fiber mode. In addition, an initial alignment with reasonable accuracy might be required to provide sufficient feedback to trigger the oscillation. Once the grating is established, however, tolerance to angular misalignment (~ a few degrees) and/or linear misalignment (~ several fiber diameters) can be expected provided the rate of changes is slower than the photorefractive response time. The photorefractive response time, however, does not limit the data rate associated with a modulated signal beam. Once the photorefractive gratings are in the steady state, the physical mechanism responsible for the coupling of the modulated laser beam into the fiber is nothing more than diffraction off a passive volume grating. From the system point of view, there is a trade-off among several performance parameters such as the degree of fault-tolerance, maximum coupling efficiency, and the recovery time. These issues require further investigations, and a detailed discussion is beyond the scope of this letter.

5. Summary and Conclusion

We have reported the first experimental demonstration of a fault-tolerant laser-to-fiber coupler using a photorefractive resonator with the fiber facet as an output coupler. Using an argon laser (514.5nm), a 45 degree-cut barium titanate crystal, and a multimode fiber, we have achieved tolerance to lateral misalignment greater than the fiber core diameter with a coupling efficiency of about 58%. Technical issues and possible techniques to improve the coupling efficiency are addressed. We also considered the extension of the method for fault-tolerant coupling of a laser diode into a singlemode fiber. In principle,

the photorefractive technique described in this paper can be applied to the coupling of light not only from a single source to a single fiber but also from multiple sources (such as one- or two-dimensional array of laser diodes, fibers, or waveguides) to a single or multiple destinations.

6. Acknowledgment

This research is supported in part by the United State Advanced Research Project Agency and Air Force Office of Scientific Research under contract No. F49620-92-C-0067.

References

1. See, for example, H.-D. Wu and F. S. Barnes, Ed., *Microlenses Coupling Light to Optical Fibers* (IEEE Press, New York, 1991).

2. Y. Makita, I. Yamauchi, K. Sono, "GRIN lenses for high efficiency coupling of laser diodes to single mode fiber," Fiber & Integrated Opt. **7**, 27-33 (1988).

3. J. Feinberg, K. R. MacDonald, "Phase-conjugate mirrors and resonators with photorefractive materials," in *Photorefractive materials and their applications II: Survey of Applications*, P. Gunter, J.-P. Huignard, Eds. (Springer-Verlag, Berlin, 1989), pp. 151-203.

4. M. Cronin-Golomb, B. Fischer, J. O. White, A. Yariv, "Passive (self-pumped) phase conjugate mirror: Theoretical and experimental investigation," Appl. Phys. Lett. **41**, 689-691 (1982).

5. J. Feinberg, "Asymmetric self-defocusing of an optical beam from the photorefractive effect," J. Opt. Soc. Am. **72**, 46-51 (1982).

6. M. Cronin-Golomb, B. Fischer, J. Nilsen, J. O. White, A. Yariv, "Laser with dynamic holographic intracavity distortion correction capability," Appl. Phys. Lett. **41**, 219-220 (1982).

7. M. Cronin-Golomb, B. Fischer, J. O. White, A. Yariv, "Passive phase conjugate mirror based on self-induced oscillation in an optical ring cavity," Appl. Phys. Lett. **42**, 919-921 (1983).

8. E. Jaatinen, and B. Luther-Davies, "Converting 10 kW multi-mode field into a single mode with a semilinear phase conjugate mirror," Int. J. of Nonlinear Optical Phys. **3**, 117-125 (1994).

9. J. A. Schuenke, "A novel technique for laser diode to single mode fiber coupling," Fiber & Integrated Opt. **6**, 191-201 (1987).

10. See, for example, M. Snowbell, N. Strasman, B. Fischer, and M. Cronin-Golomb, "Efficient self-aligning multibeam coupling into a single-mode fiber," J. of Lightwave Tech. **13**, 55-61 (1995), and the references cited therein.

11. K. O. Hill, B. Malo, F. Bilodeau, and D. C. Johnson, "Photosensitivity in optical fibers," Ann. Rev. Mater. Sci. **23**, 125-157 (1993).

12. M. Cronin-Golomb, "Infrared photorefractive passive phase conjugator with $BaTiO_3$: Demonstration with GaAlAs and 1.09-μm Ar^+ lasers," Appl. Phys. Lett. **47**, 567-569 (1985).

13. R. B. Bylsma, A. M. Glass, D. H. Olson, "Optical signal amplification at 1.3μm by two-wave mixing in InP:Fe," Electron. Lett. **24**, 360-362 (1988).

14. J. Strait, J. D. Reed, A. Saunders, G. C. Valley, M. B. Klein, "Net gain in photorefractive InP:Fe at λ=1.32μm without an applied field," Appl. Phys. Lett. **57**, 951-953 (1990).

15. A. Partovi et al., "Photorefractivity at 1.5 μm in CdTe:V," Appl. Phys. Lett. **57**, 846-848 (1990).

Figure Captions

Fig. 1 A schematic illustration of a photorefractive semilinear phase conjugate resonator (PSPCR)

Fig. 2 An experimental configuration for fault-tolerant laser-to-fiber coupling using a photorefractive semilinear phase conjugate resonator with the fiber facet as an output coupler. Loss of optical power (in dB) in each stage is indicated in the lower part of the figure.

Fig. 3 Experimental results showing fault-tolerant coupling. The upper and the lower traces correspond to output signals from detectors D1 and D2, (i.e., the transmitted and the phase conjugate signals), respectively.

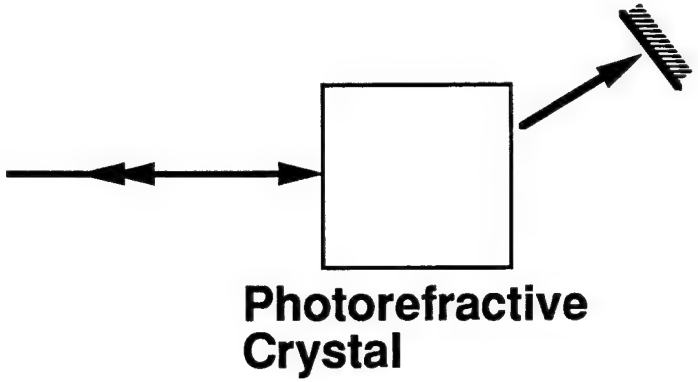

Fig. 1

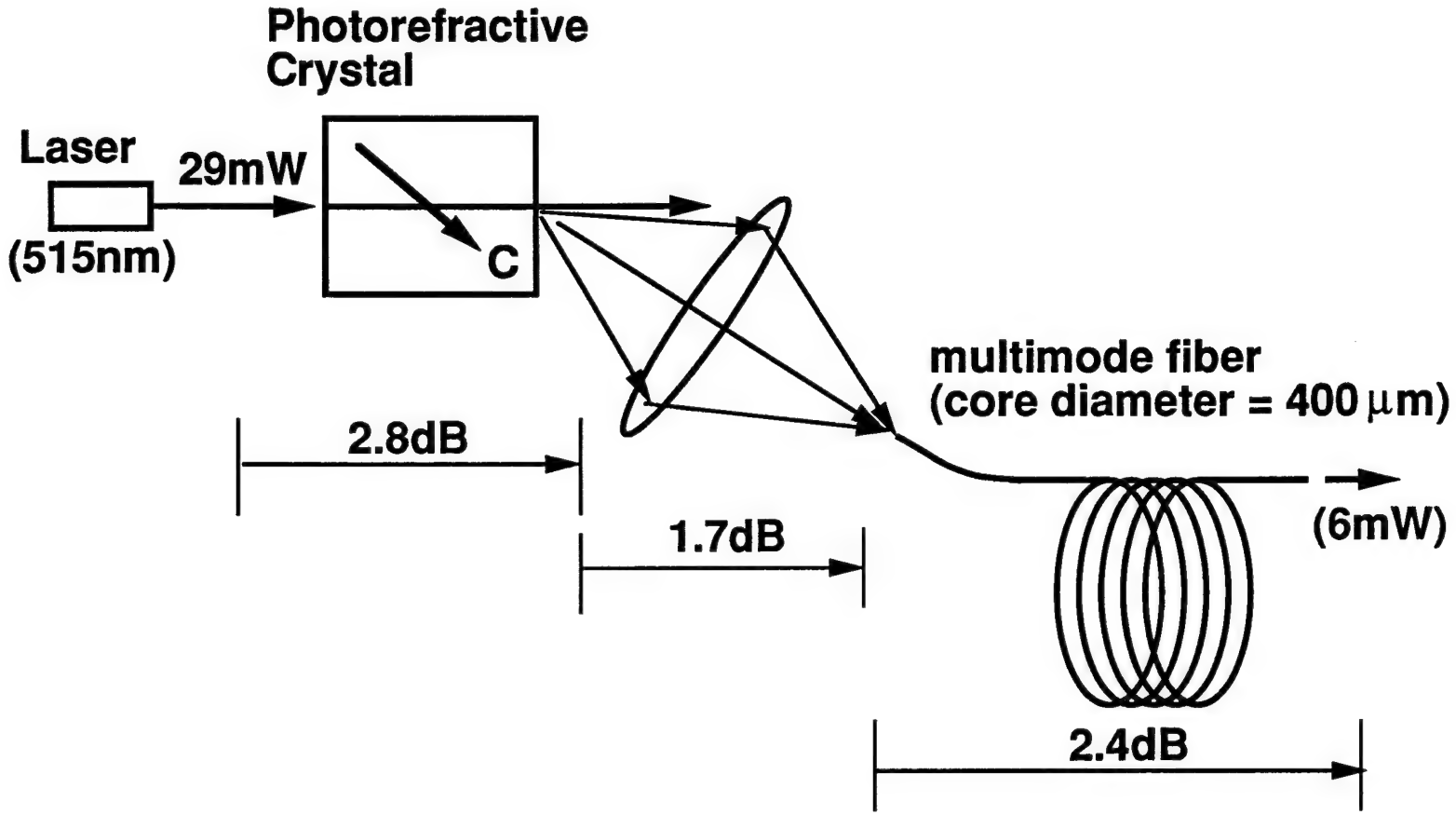
Photorefractive
Crystal
Laser
29mW
(515nm)
C
multimode fiber
(core diameter = 400 μm)
2.8dB
1.7dB
(6mW)
2.4dB

Fig. 2

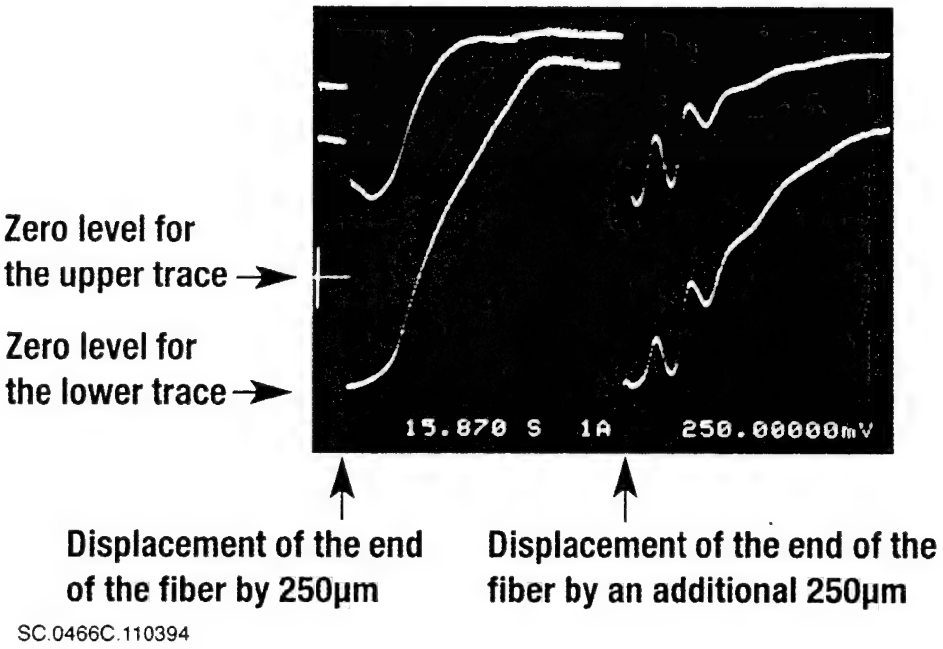
Zero level for
the upper trace
Zero level for
the lower trace
15.870 S 1A 250.00000mV
Displacement of the end
of the fiber by 250µm
Displacement of the end of the
fiber by an additional 250µm
SC.0466C.110394

Fig. 3

Appendix 6.4

A. Chiou, P. Yeh and C. Gu, "A photorefractive spatial mode converter for multimode to singlemode fiber-optic coupling", to appear in *Opt. Lett.* May 1995.

A Photorefractive Spatial Mode Converter for Multimode to Singlemode Fiber-Optic Coupling

Arthur Chiou
Rockwell Science Center
1049 Camino Dos Rios, Thousand Oaks, CA 91362
Tel:(805)373-4464, Fax:(805)373-4774
Internet:aechiou@scimail.remnet.rockwell.com

Pochi Yeh, Changxi Yang
Electrical Engineering Dept., University of California at Santa Barbara
Santa Barbara, CA 93106

Claire Gu
Electrical & Computer Engineering Dept., Penn State University
University Park, PA 16802

Abstract

We report the first experimental demonstration of a photorefractive spatial mode converter (based on mutually-pumped phase conjugation) which couples light efficiently from a multimode fiber into a singlemode fiber with an extremely large degree of tolerance to misalignment. Using an argon laser (514.5nm) and a barium titanate crystal, we have demonstrated that the laser light can be coupled from a multimode fiber (core diameter = 100μm, numerical aperture = 0.37) into a singlemode fiber (core diameter = 2.9μm, numerical aperture = 0.11), with an efficiency of about 15%, and with an alignment tolerance of about 100 μm. The coupling efficiency is more than two orders of magnitude, and the tolerance to misalignments is more than 30 times better than the corresponding values achievable by conventional techniques.

A Photorefractive Spatial Mode Converter For Multimode to Singlemode Fiber-Optic Coupling

Arthur Chiou
Rockwell Science Center
1049 Camino Dos Rios, Thousand Oaks, CA 91362
Tel:(805)373-4464, Fax:(805)373-4774
Internet:aechiou@scimail.remnet.rockwell.com

Pochi Yeh, Changxi Yang
Electrical Engineering Dept., University of California at Santa Barbara
Santa Barbara, CA 93106

Claire Gu
Electrical & Computer Engineering Dept., Penn State University
University Park, PA 16802

Conventional techniques using a single- or multiple- lens system for coupling of light from a multimode fiber (MMF) to a singlemode fiber (SMF) suffer from two major technical difficulties. 1. The coupling efficiency is inherently low; the maximum coupling efficiency is fundamentally limited to 1/N where "N" is the number of spatial modes at the exit end of the multimode fiber, assuming that the energy is uniformly distributed among all the "N" modes. 2. The coupling efficiency is extremely sensitive to alignment. In this letter, we present the principle of operation and the first experimental demonstration of a photorefractive spatial mode converter which is capable of coupling light from a MMF into a SMF with a coupling efficiency that can be two to three orders of magnitude higher than the "1/N" limit. In addition, it is self-adaptive and hence can tolerate a fair amount of angular and/or lateral misalignments.

The novel technique for efficient and fault-tolerant coupling of light from a MMF into a SMF is based on photorefractive mutually-pumped phase conjugation (MPPC).[1] When two laser beams (of the same color, but mutually incoherent) with appropriate wavelengths and polarizations enter a photorefractive crystal at proper angles, gratings are generated by each incident beam via interference with its own scattered components. Under appropriate conditions, only the set of gratings that transforms each beam into the phase conjugate of the other survives the cross-erasure. As is illustrated in Fig. 1, such a

phenomenon, know as mutually-pumped phase conjugation (or MPPC),[1] can transform spatial wavefront of a multimode beam (designated the signal beam in Fig. 1) to match that of a singlemode beam (designated the beacon beam in Fig. 1) and couple it efficiently (much higher than 1/N) into a SMF. When the fibers are displaced from the optimum position/orientation, a new set of gratings that corrects for the changes is self-generated provided that the two beams remain intersecting (or overlapping) inside the crystal. As a result of this self-healing process, the technique can tolerate a large amount of angular and lateral misalignments. In sharp contrast, conventional techniques using single- or multiple- lens system for multimode to singlemode coupling are so sensitive to both angular and lateral alignment that it is extremely difficult to align the system and hold the coupling efficiency at a steady and significant level. Although many features of MMPC of two or more Gaussian beams in a wide variety of configurations and context have been studied and reported,[1,2,3,] to the best of our knowledge, this letter reports the first successful experimental demonstration of its application for efficient and fault-tolerant multimode to singlemode fiber-optic coupling.

The experimental configuration is illustrated schematically in Fig. 2. The output from an argon laser (514.5nm) is split into two by a variable beam splitter, consisting of a half-wave plate ($\lambda/2$) and a polarizing beam splitter cube (PBS1). One of the beams (the beacon beam with horizontal polarization) is focused into a SMF (core diameter d = 2.9μm, NA = 0.11, length = 10m) via a microscope objective (MO1, 20x, NA = 0.40) and a five-axis SMF aligner/holder (FH1), while the other beam (the signal beam with vertical polarization) is focused into a MMF (core diameter D = 100μm, numerical aperture NA = 0.37 length = 4m) via another microscope objective (MO2, 10x, NA = 0.25). Using this arrangement, we typically achieve a coupling efficiency of about 60% for the SMF and 80% for the MMF. Although the signal beam injected into the MMF is vertically polarized, the polarization is severely scrambled by the MMF, rendering the output essentially unpolarized. A linear polarizer (P) is used to filter out the vertically-polarized component and transmit only the horizontal component which is collected and focused by Lens L1 (focal length = 38mm, f/ = 0.7) into a 45°- cut barium titanate crystal (BT) as shown in Fig. 2. At the exit face of the crystal the signal beam fans[4] strongly towards the c-axis (indicated by an arrow in Fig. 2) of the crystal. The fanning beam is collected and loosely focused by a second lens L2 (focal length = 38mm, f/ = 0.7). The other end (facet) of the SMF (which is mounted on another five-axis fiber holder, FH2) is then placed approximately at the focal point of the multimode beam and oriented so that the two beams (signal and beacon) intersect inside the crystal. The interaction of the two

beams inside the crystal leads to mutually-pumped phase conjugation[1,5] which not only efficiently (and adaptively) transforms the speckle pattern of the multimode output into the bell-shape intensity distribution of the SMF but also directs the transformed beam into the SMF (Fig. 1). Since the transformed beam is automatically mode-matched to that of the SMF (as a result of the phase conjugation process), the coupling efficiency (which is essentially limited by the diffraction efficiency of volume gratings responsible for the MPPC) can be very high. Two shutters (SH1 and SH2) are used to switched ON/OFF the two input beams, and two detectors (D1 and D2) are used to monitor the vertical and horizontal polarization components of the signal beam originated from the MMF, transmitted through the SMF and sampled by a polarizing beam splitter (PBS2) and a beam splitter (BS), respectively.

For a given photorefractive crystal and a specific experimental geometry, the multimode to singlemode coupling efficiency depends on the beacon-to-signal power ratio. In our experiment, the optical power of the two beams injected into the crystal was varied in the range of 1mW to 20mW. A typical set of experimental data as depicted in Fig. 3 reveals the following points. 1. The polarization of the transmitted light is essentially horizontal (i.e., the polarization is preserved in the mode conversion and the transmission through the SMF). 2. The coupling efficiency peaks when the beacon-to-signal power ratio is around 2, and decreases as the ratio increases. The maximum coupling efficiency achieved is about 15%. Another interesting point that is not apparent in Fig. 3 is that when the ratio is reduced to less than one, the coupling becomes unstable.

When the beacon beam was switched off (by shutter SH1 in Fig. 2), the signal transmitted through the SMF (as monitored by the detector D1) decayed slowly (~ a few seconds) as the photorefractive gratings responsible for the coupling were erased by the signal beam. The signal recovered at a much faster rate (in less than 1 second) when the beacon beam was switched on again, provided that the gratings were not severely erased (Fig. 4a). To further illustrate this point, an example in which the beacon beam was turned off for about 80 seconds was shown in Fig. 4b. In this example, the gratings were erased to such an extent that the coupling efficiency was reduced to less than 0.01% of the maximum value; the corresponding recovery time was much longer. The contrast ratio (i.e., the maximum transmitted power at the steady state / minimum transmitted power after the beacon beam is turned off and the gratings responsible for MPPC are completely erased) which is limited by the background stray light is greater than 10^5.

To demonstrate the degree of fault-tolerance of this novel coupling technique, the facet of the SMF was displaced horizontally by adjusting one of the micrometers of the five-axis fiber holder (FH2 in Fig. 2). The transmitted signal (as monitored by the output of D1 and shown in Fig. 5) dropped abruptly and recovered slowly (~ 40seconds) as the original gratings were erased and new gratings were formed. The minima of the signal level in Fig. 5 was limited by the back reflection of the beacon beam from the microscope objective (MO1) and the SMF. We observed a complete recovery of signal via self-healing even when the fiber facet was displaced by about 100μm which is more than 30 times the fiber core diameter. Likewise, we have also varied the vertical position and the angular orientation of the fiber facet and show that signal recovery applies to all degrees of freedom.

The 1/N limit for the coupling of light from a MMF into a SMF using the conventional technique (such as a single- or multiple- lens system) can be estimated by $(d/D)^2$, where d and D are the core diameters of the SMF and the MMF, respectively. For d = 2.9μm and D = 100μm, $(d/D)^2 \sim 0.084\%$. To compare with this crude estimation, a microscope objective (10x, NA = 0.30) was used to couple the output of the MMF directly into the SMF (mounted on the same five-axis fiber holder/aligner, FH2). The coupling efficiency was so sensitive to the position of the facet of the SMF that it was extremely difficult to maximize the output and hold the fiber facet at the optimum position. Typically, the coupling efficiency achieved was in the range of 0.01% to 0.06%. In contrast, the photorefractive technique described above consistently exhibits a coupling efficiency of about 15%, which is more than two orders of magnitude higher than the 1/N limit !

In summary, we have proposed and successfully demonstrated a novel technique based on MPPC for efficient and fault-tolerant coupling of a laser light from a multimode into a singlemode fiber. We have achieved a coupling efficiency of about 15% and tolerance to lateral misalignment of about 100μm. The former is more than two orders of magnitude higher (and the latter more than 30 times higher) than the corresponding values achievable by conventional techniques.

This research is supported by ARPA/AFOSR under contract No. F49620-92-C-0067.

References

1. See, for example, Q. B. He, in *Photorefractive Materials, Effects, and Applications*, P. Yeh, C. Gu, Eds. (SPIE, Bellingham, 1993), pp. 59-75, and the references cited therein.
2. S. Weiss, S. Sternklar, and B. Fischer, Opt. Lett. **12**, 114 (1987).
3. Q. C. He, J. Shamir, and J. G. Duthie, Appl. Opt. **28**, 306 (1989).
4. J. Feinberg, J. Opt. Soc. Am. **72**, 46 (1982).
5. P. Yeh, Appl. Opt. **28**, 1961 (1989).

Figure Captions

Fig. 1 A schematic illustration of a photorefractive mode converter (based on mutually-pumped phase conjugation) that can couple light efficiently from the output of a multimode fiber into a singlemode fiber.

Fig. 2 An experimental configuration for the demonstration of fault-tolerant and efficient coupling of light from a multimode fiber into a singlemode fiber. $\lambda/2$: half-wave plate, PBS: polarizing beam splitter, SH: shutter, BS: beam splitter, D: detector, MO: microscope objective, FH: fiber holder, SMF: singlemode fiber, MMF: multimode fiber, M: mirror, BT: barium titanate crystal, L: lens, BB: beam blockage, P: polarizer.

Fig. 3 Multimode to singlemode light coupling efficiency as a function of the power ratio of the beacon and the signal beams.

Fig. 4 Oscillograms showing the decay and the recovery of the signal transmitted through the singlemode fiber when the beacon beam was switched off and on again at an instant when the transmitted power was (a) 54%, (b) 0.01% of the peak value.

Fig. 5 Oscillograms showing the abrupt drop and the gradual recovery of the signal transmitted through the singlemode fiber when the fiber facet was displaced horizontally. The minima of the signal level represent the background due to back reflection of the beacon beam from the microscope objective and the fiber.

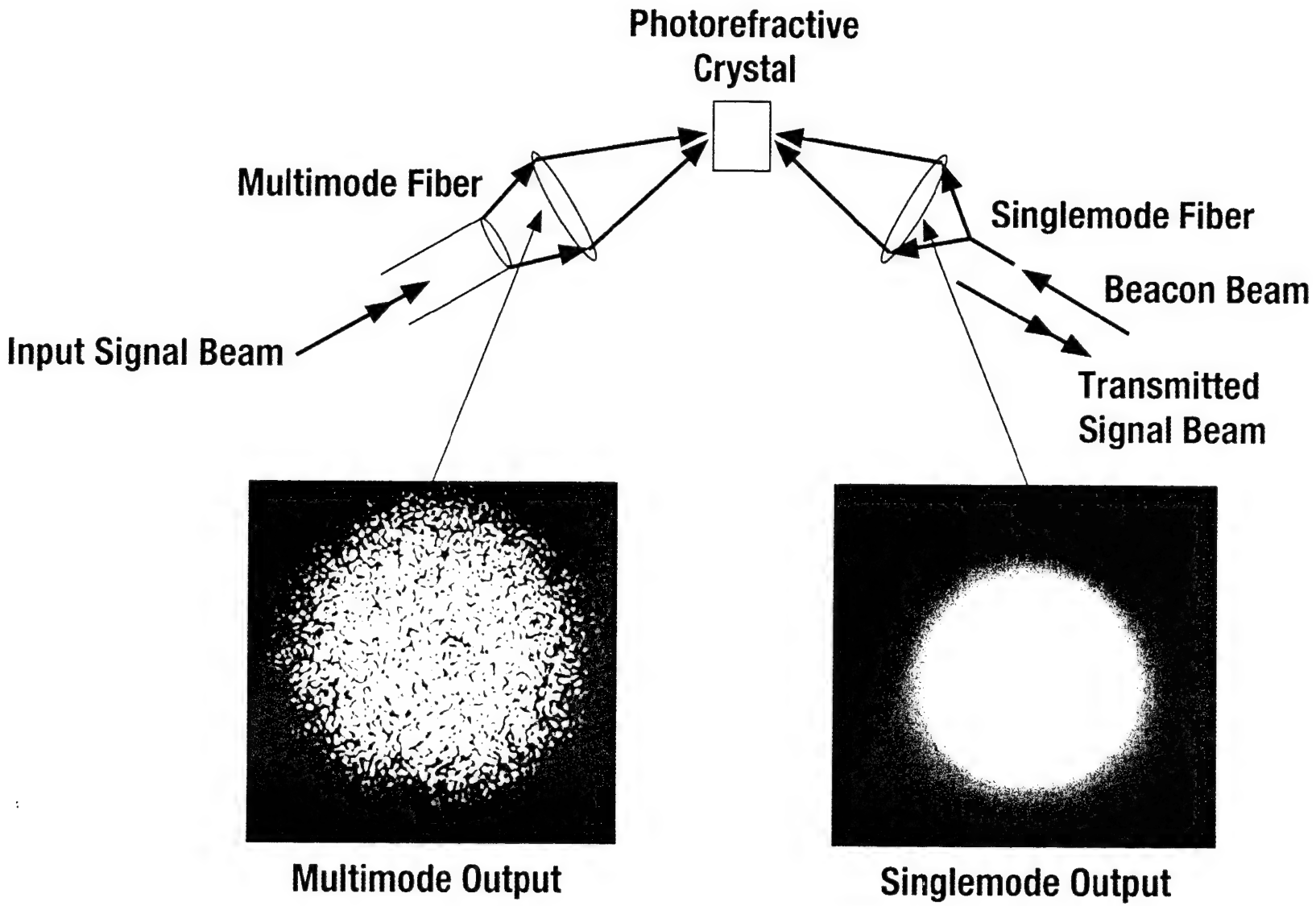

SCP.1093E.121394

65
C13086D/ejw

Fig. 1
"A Photorefractive Spatial
Mode Converter for ....."
A. Chiou, et al.

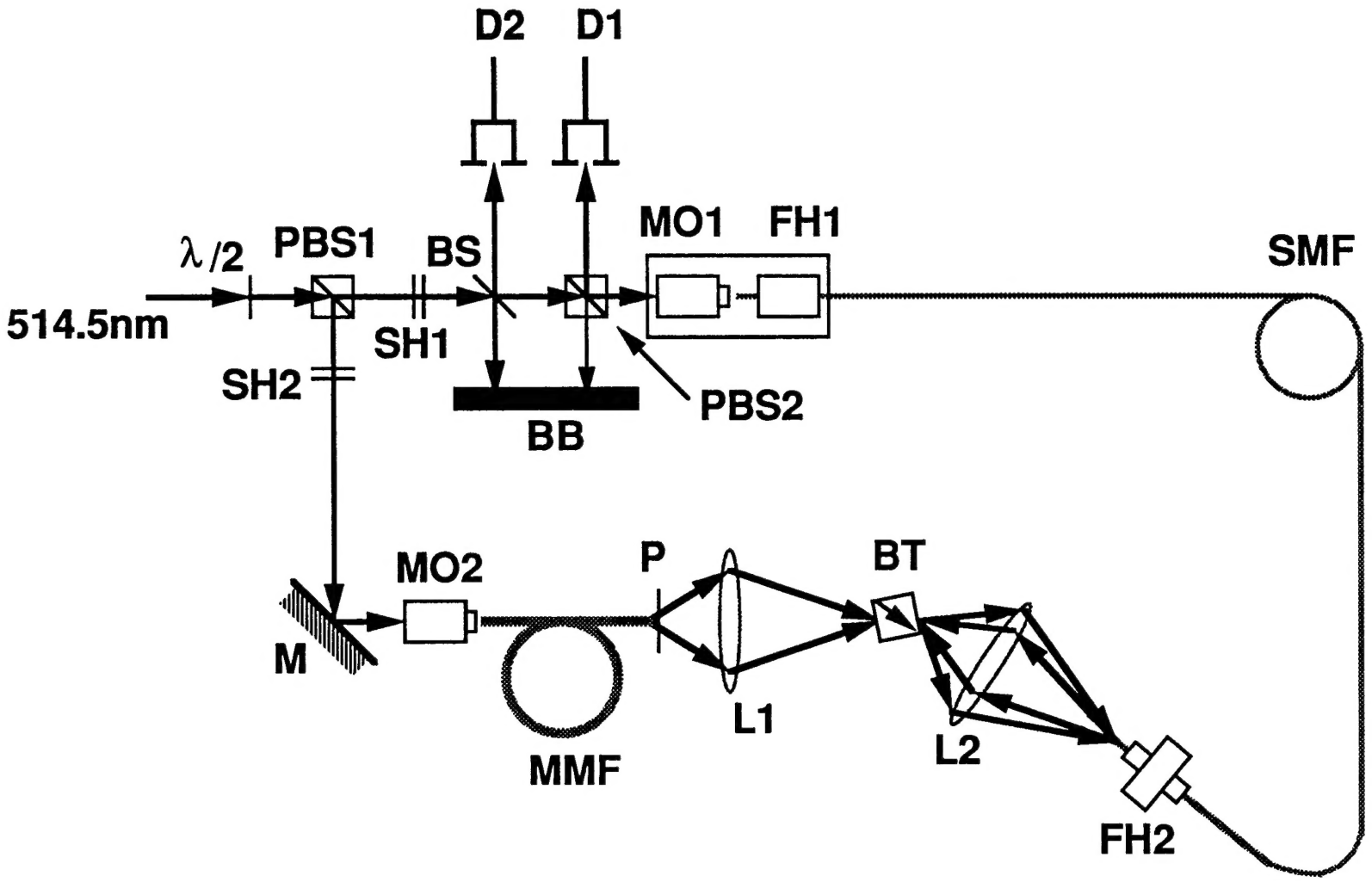

Fig. 2
"A Photorefractive Spatial Mode Converter for ....."
A. Chiou, et al

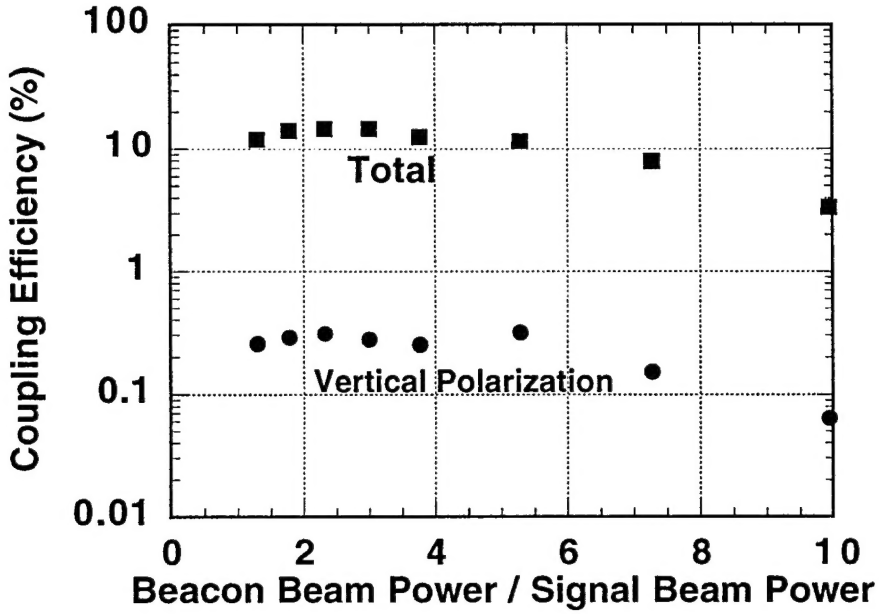

Fig. 3
"A Photorefractive Spatial
Mode Converter for ....."
A. Chiou, et al.

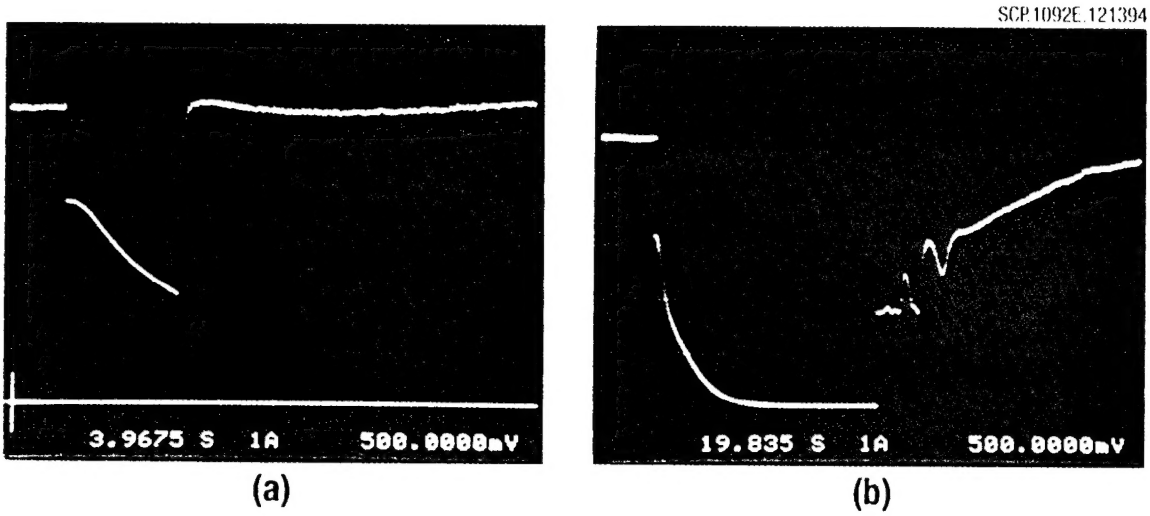

(a) (b)

Fig. 4
"A Photorefractive Spatial Mode Converter for ....."
A. Chiou, et al.

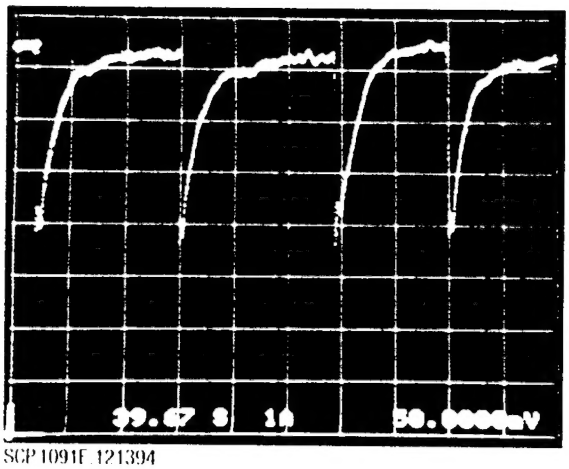

Fig. 5
"A Photorefractive Spatial
Mode Converter for ....."
A. Chiou, et al.